

Advances in Chip-Scale Quantum Photonic Technologies

Liangliang Lu,* Xiaodong Zheng, Yanqing Lu,* Shining Zhu,* and Xiao-Song Ma*

Quantum photonic system has made remarkable achievements in computing and communication. Serving as quantum information carriers, photons are flying qubits and robust against decoherence, emerging as a desirable platform to make quantum processor a reality. However, with system's complexity and functionality scaling up, the requirements for stability, programmability, and manufacturability will be in high demand. Integrated photonics, compatible with complementary metal-oxide-semiconductor fabrication, has overwhelming dominance in terms of density and performance, making it an unrivaled contender for large-scale quantum information processing (QIP). To improve the performance of individual blocks and integrate them on a common substrate is one of the core tasks for a practical quantum processor. Here, the recent advances in components that constitute quantum photonic systems on silicon photonics platform, including sources, modulators, and detectors are reviewed. Burgeoning quantum photonics applications, such as multi-dimensional, multi-photon QIP and integrated quantum key distribution are highlighted.

1. Introduction

The properties of quantum superposition and entanglement, promise that QIP technologies are in essence more powerful than classical counterparts, such as quantum-enhanced computing,^[1] communications,^[2] and metrology.^[3] After years of in-depth theoretical and experimental studies, the development of QIP is now at a critical state, manifested in offering powerful

solutions to some complex problem^[4–7] and building global quantum network.^[8,9] Based on the framework of binary quantum system, we can encode information in a general quantum bit (or qubit) state of the form $\alpha|0\rangle + \beta|1\rangle$, where α and β are complex numbers. In principle, any two-level quantum system can represent a qubit.

Photonic qubits are ideal carriers for quantum information science. On one hand, they do not suffer from decoherence due to weak coupling to the surroundings and can be easily controlled with high fidelity without requiring hard-to-reach operating conditions.^[10] On the other hand, photons as flying qubits are particularly advantageous for quantum information tasks between distant locations, such as networking QIPs^[11,12] and quantum communication.^[13] To date, various efficient ways of optical quantum computing have been developed.^[14–17] The Knill, Laflamme, and Milburn (KLM) scheme^[14]

and the cluster-state based one-way quantum computing^[18] motivated worldwide efforts toward universal quantum computation with photons. However, it is inevitable that as the complexity of computation grows, large numbers of photonic qubits and gates are needed. Moreover, the technological scalability and phase stability as well as reconfigurability become increasingly important. By leveraging advances in complementary metal-oxide-semiconductor (CMOS) fabrication techniques for microprocessors and classical communications, integrated photonic circuits become a more appealing platform for future quantum technologies compared with bulk-optical systems. They have shown great potential for realizing system integration and performance required by QIP.^[19–26]

Generally, integrated quantum photonic information processor demands three functions: efficient generation of on-demand quantum states, their manipulation in various degrees of freedom, and single photon detection. Different material platforms have their own strengths to realize the three functions individually or partially. For example, lithium niobate, an emerging material which is studied in integrated photonics,^[27] is becoming a leading and flexible platform for integrated photon pair sources^[28] and high-speed modulators.^[29,30] Femtosecond-laser-written waveguides are formed by using high peak power femtosecond pulse to cause localized nonlinear absorption, which changes the refractive index and thus builds a waveguide between the focus and substrate. The laser can be focused at different depths inside the material, allowing the realization of layered waveguide arrays for the study of 3D interferometric networks.^[31] Niobium nitride nanowire on sapphire substrate

L. Lu, X. Zheng, Y. Lu, S. Zhu, X.-S. Ma
National Laboratory of Solid-State Microstructures
School of Physics, College of Engineering and Applied Sciences
Collaborative Innovation Center of Advanced Microstructures
Nanjing University
Nanjing 210093, China
E-mail: lianglianglu@nju.edu.cn; yqlu@nju.edu.cn; zhusn@nju.edu.cn;
xiaosong.ma@nju.edu.cn

L. Lu
Key Laboratory of Optoelectronic Technology of Jiangsu Province
School of Physical Science and Technology
Nanjing Normal University
Nanjing 210023, China

 The ORCID identification number(s) for the author(s) of this article can be found under <https://doi.org/10.1002/qute.202100068>

© 2021 The Authors. Advanced Quantum Technologies published by Wiley-VCH GmbH. This is an open access article under the terms of the Creative Commons Attribution-NonCommercial-NoDerivs License, which permits use and distribution in any medium, provided the original work is properly cited, the use is non-commercial and no modifications or adaptations are made.

DOI: 10.1002/qute.202100068

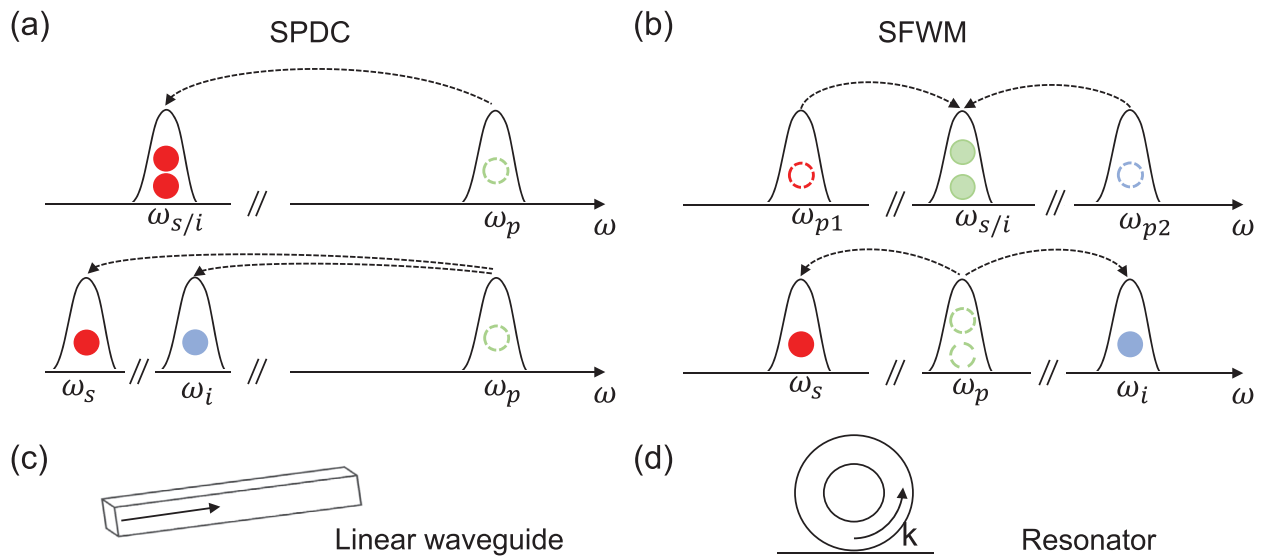


Figure 1. a) Conceptual scheme of the spontaneous parametric down conversion (SPDC) and spontaneous four-wave mixing (SFWM), with the generated signal and idler photons in the same (up) or different frequency (down) modes. Two popular methods for generating photon pairs, that is, c) linear waveguide and d) microring resonator.

was demonstrated as a single-photon sensitive superconducting device two decades ago.^[32] Since then, superconducting nanowire single-photon detectors (SNSPDs) have been an attractive device for photon counting.

Many other material platforms have also attracted much attention, such as diamond,^[33] silicon carbide,^[34] and III–V semiconductors.^[35,36] Among them, nanostructures on silicon substrate is arising as an outstanding platform for the development of quantum photonic technology. Using high nonlinearity and reconfigurable routing architectures, it allows phase-stable quantum systems implementing on $\approx \text{cm}^2$ scale with core functionalities listed above. It has been used to prepare an integrated quantum photonic device with hundreds of components, realizing the generation, manipulation and analysis of high-dimensional entangled states,^[37] and some quantum tasks such as quantum sampling^[25,38] and chip-based quantum communications.^[39–42] Furthermore, it is advantageous to use silicon as a cost-effective large-diameter substrate for device production, as CMOS compatible fabrication makes it easy to interface with silicon microelectronics for reducing total device footprint, weight and power.^[43,44] However, there remain many challenges, for example making high-quality photon source and high-fidelity quantum logic operations, reducing losses from components and improving photon detection, and more particularly integrating high-performance components monolithically on a common substrate. Here we will review the progress of quantum devices and technologies with a focus on platforms on silicon substrate that we think are indispensable for realistic large-scale QIP. On the basic devices side, we mainly introduce the recent progress of several material platforms in the key functions of photonic quantum states generation, modulation and detection, and illustrate their strength and weakness to show the great potential of hybrid circuits as compared with monolithic circuits. As to the applications, we concentrate on the latest research on system-level integration of multi-dimensional

and multi-photon QIPs and routes toward fully-integrated QKD. Comprehensive reviews of silicon quantum photonics chip can be found in refs. [44, 45], while device- and platform-related reviews can be referred to refs. [20–22, 46].

2. Integrated Quantum Photonic Devices

2.1. Quantum Light Source

Quantum light source is an essential resource for a wide range of quantum-enhanced technologies and foundational tests of quantum mechanics.^[47–49] Photons produced with high quality, such as near unity indistinguishability, purity, and entanglement fidelity, are mainly being developed in two classes: deterministic single photon emission based on quantum dots (QDs)^[50–52] and nonlinear parametric processes relied on probabilistic sources. In this review, we focus on the second approach. The second ($\chi^{(2)}$) or third order ($\chi^{(3)}$) based nonlinear processes, termed as spontaneous parametric down conversion (SPDC) or spontaneous four wave mixing (SFWM), providing significant advantages and remaining an efficient way to generate photon states at room temperature. For SPDC or SFWM, either one (Figure 1a) or two pump photons (Figure 1b) are annihilated to produce a pair of signal and idler photons. They have common generation mechanism, only virtual photons provided by vacuum fluctuations satisfy energy and momentum conservation conditions can be transformed into real. Depending on the pump configuration, the photon pairs can be generated with two same (in the top half of Figure 1a,b) or different (in the bottom half of Figure 1a,b) frequencies, satisfying energy conservation

$$\text{SPDC : } \begin{cases} \omega_p = 2\omega_{s/i} & (\text{Degenerated}) \\ \omega_p = \omega_s + \omega_i & (\text{Nondegenerated}) \end{cases} \quad (1)$$

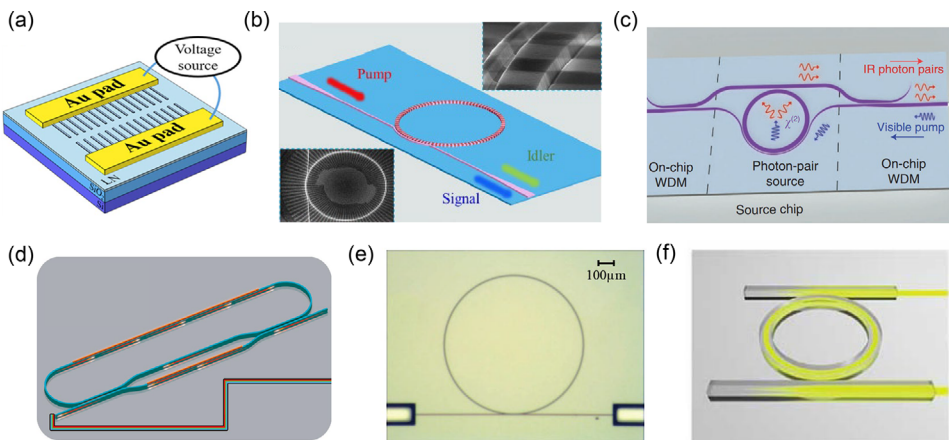


Figure 2. Examples of integrated SPDC and SFG photon pair sources. a) Periodic-poling thin-film lithium niobate waveguide. Reproduced with permission.^[55] Copyright 2021, American Physical Society. b) Thin-film lithium niobate microresonator. Reproduced with permission.^[56] Copyright 2020, American Physical Society. c) Aluminum nitride microresonator. Reproduced with permission.^[57] Copyright 2017, The Authors, published by Springer Nature under the terms of a Creative Commons Attribution-NonCommercial-NoDerivs 4.0 International License. d) MZI-based silicon MRR. Reproduced with permission.^[62] Copyright 2020, Optical Society of America. e) Silicon nitride microresonator. Reproduced with permission.^[63] Copyright 2018, Optical Society of America. f) High-index doped silica microresonators. Reproduced with permission.^[58] Copyright 2016, American Association for the Advancement of Science (AAAS).

or

$$\text{SFGM} : \begin{cases} \omega_{p1} + \omega_{p2} = 2\omega_{s/i} & (\text{Degenerated}) \\ 2\omega_p = \omega_s + \omega_i & (\text{Nondegenerated}) \end{cases} \quad (2)$$

with ω_j ($j = p, p1, p2, s, i$) being the frequencies of the pump, signal and idler photons. The popular integrated sources for generating photon pairs are linear waveguides and microring resonators (MRRs), as sketched in Figure 1c,d.

2.1.1. Photon Pair Source

Second-order nonlinear waveguides can yield photon pairs with the application of quasi-phase-matching (QPM). In recent years, lithium niobate thin film on insulator (LNOI), was developed as a compelling platform for integrated nonlinear photonics.^[53–56] Using a LNOI chip, ultrabright entangled photons have been produced in a bandwidth of 130 nm by using group velocity dispersion and domain engineering (Figure 2a).^[55] The high refractive index contrast in LNOI provides improved confinement of optical signals, inducing photon pair generation rate over two orders of magnitude compared to existing technologies.^[54,55] However, these waveguides normally require mm- or cm-length to guarantee the photon rate, which limit high-density integration. In contrast to linear waveguides, MRRs have a much smaller footprint than linear waveguides, allowing not only much narrower bandwidth filtering but also higher efficiency due to the field enhancement, thereby reducing the requirements for pump power at a given rate.^[45,56–59] This helps because the pump power required in MRR is significantly higher than that of generated photons, placing strict requirements to suppress the pump noise. Normally, a MRR consists of a looped optical waveguide and a coupling nanowire waveguide to access the loop. When the optical fields acquire an integer times 2π phase shift after a round trip, the fields interfere constructively and the cavity is in resonance,

with a wavevector separation of $\frac{2\pi}{L}$, where L is the geometric length of the ring. The quality factor (Q) is often used to describe the MRR performance, where $Q = \lambda/\Delta\lambda$ with λ the resonance wavelength and $\Delta\lambda$ the full width half maximum in wavelength, respectively. The total Q is jointly determined by the intrinsic (Q_i) and external (Q_e) quality factors by^[60]

$$1/Q = 1/Q_i + 1/Q_e \quad (3)$$

where

$$Q_i = \frac{\omega}{\alpha v_g} \quad (4)$$

and

$$Q_e = \frac{\omega L}{|k|^2 v_g} \quad (5)$$

where α is the round-trip loss coefficient in the cavity, v_g is the group velocity of the light, ω denotes the angular frequency of the light and k is the coupling coefficient between the ring and bus waveguides. In experiments, these three Q factors are usually estimated by the transmission spectrum near the resonance wavelength if they are much larger than 1. The extinction ratio (γ) can be expressed as^[61]

$$\gamma \approx \left| \frac{Q_i - Q_e}{Q_i + Q_e} \right|^2 \quad (6)$$

The MRR can be in over, critical and under coupling states if $Q_i > Q_e$, $Q_i = Q_e$ and $Q_i < Q_e$, respectively.

Recently, concentric periodic-poling MRR has been demonstrated on a LNOI chip to create high-quality photon pairs over multiple wavelength channels.^[56] The heralded generation rate can be tens of megahertz (MHz) with only microwatt pump power. To realize good coupling for all optical modes with

large frequency separation between pump and signal/idler photons, a pulley waveguide has a role of the ring-bus waveguide coupler (Figure 2b). Similarly, the dispersion engineering has been demonstrated in a $\chi^{(2)}$ aluminum nitride MRR with a narrow pulley waveguide and wider bus waveguide for visible and telecom photons respectively (Figure 2c).^[57] The QPM is achieved for high-order transverse-magnetic (TM_2) pump mode and fundamental TM (TM_0) signal and idler modes, implying MHz photon pair generation rates.

Although the nanoscale $\chi^{(2)}$ waveguides can produce photon pairs efficiently, they have yet to reach their full potential for system level applications. Silicon waveguides are appealing for scale-up QIP owing to the existing foundry infrastructure. Due to centrosymmetric crystalline structure, silicon waveguides do not possess $\chi^{(2)}$ but has relatively large $\chi^{(3)}$ due to tight modal confinement, enabling efficient nonlinear photonic interaction of modes therein at moderate pump power. Meanwhile, the narrowband spontaneous Raman scattering noise is separated from the pump frequency by 15.6 THz, which makes it easy to be suppressed.^[64] Generally, the phase matching bandwidth of the photons generated from waveguides is broad, and narrow-band-pass filters need to be used to obtain high-quality photons.^[37,38,65–70] In MRRs, phase matching condition is naturally satisfied due to signal and idler evenly spaced relative to the pump at specific resonance wavelengths. Multiple types of silicon MRR sources have been investigated.^[61,71–79] For continuous wave pump in a single-bus MRR, the optimal conditions for highest rate or brightness of photon pairs correspond to overcoupling ($Q_e/Q_i = 3/4$) or critical coupling ($Q_i = Q_e$), respectively.^[76] Nevertheless, the ring's coupling and loss are sensitive to fabrication process, a slight variation of the coupling coefficient can impact the generation rate significantly. Ref. [80] demonstrated that the operating point of a MRR can be controllable by employing a tunable evanescent field coupler, exhibiting a quasi-continuously Q factors between 9000 and 96 000. Burridge et al. used Mach-Zehnder interferometer (MZI) based MRR to realize tunable Q factor in a similar way (Figure 2d).^[62] From the simulations, Q_i has more of an impact than Q_e on photon pair generation rate.^[76] To improve the rate, low round-trip loss, which is mainly induced by the side-wall roughness and bending loss, is preferred. An ultrahigh- Q ($>10^6$) MRR has been realized with uniform multimode silicon waveguides,^[81] where the fundamental mode can propagate in the multimode racetrack resonator with ultralow loss.

Despite impressive demonstrations, attention should be paid to the parasitic nonlinear effects in silicon, such as two-photon absorption (TPA) and free carrier absorption (FCA), as the pump power increases. They may damage the pair generation properties.^[64,82] FCA contributed by the TPA-excited electrons can be eliminated by using a lateral p-i-n junction across the waveguide to drive the free carriers out of the waveguide.^[83] Nevertheless, TPA imposes a strong limit to silicon source operating at telecom band and its effect on single photon generation has been demonstrated in single bus MRR.^[84] The optional solution is to move the pump wavelength to a regime where the bandgap is too large for TPA.^[85]

Alternatively, silicon nitride (Si_3N_4)^[59,63,86–88] and high-index doped silica (Hydex)^[58,89,90] exhibit no TPA and can be operated at high laser power although their nonlinear indexes are smaller

than those in silicon. In contrast to silicon, Si_3N_4 and Hydex exhibit lower propagation loss and broader transparency window ranging from ultraviolet to mid-infrared. Resonators in Si_3N_4 and Hydex are excellent candidates for integrated quantum light generation when the pump power is kept below the threshold of parametric oscillation. Entanglement in frequency degrees of freedom (DOF) with a coherent superposition of several frequency bins has been verified in Si_3N_4 (Figure 2e)^[63] and Hydex,^[89] respectively. Sideband modulation has been used to coherently mix the neighboring frequency modes, avoiding the difficulty in high timing resolution for temporal correlation measurement. By engineering the dispersion properly, photon pairs with spectral translation range from visible to telecommunication wavelengths have been realized based on Si_3N_4 resonators,^[59] likely to be a promising tool to link different quantum systems for a variety of applications in networking and sensing. It has also been demonstrated that quantum frequency combs can be generated in Hydex with several bi- and multiphoton entangled qubits and directly applied for quantum communication and computation (Figure 2f).^[58]

2.1.2. Single Photon Source

Single photon source is preferable in many applications, such as quantum cryptography and quantum computing. An ideal single photon source needs to meet two criteria: 1) deterministically, that is, it can be generated on demand, and there is only one single photon output at a time; 2) indistinguishability, that is, subsequent emitted photons are identical and in a desired single mode. While there is no source can fully satisfy the requirements, the research has been carried out in several physical systems,^[91–94] among which the representative are “deterministic” QDs and “probabilistic” parametric sources. We want to emphasize that although the difference between “deterministic” and “probabilistic” is clear in concept, the distinction is equivocal in practical application. For example, when extracting photons from a “deterministic” source, there is often a nonnegligible loss. With the increase of extraction loss, the theoretically deterministic source reduces to probabilistic in practice. Consequently, high-efficiency hybridly integrate QDs onto waveguides or cavities is attractive. Recently, significant efforts have been made to couple QDs and photonic structures efficiently,^[95] control position,^[96] and frequency^[97] of (multiple)^[98] QDs precisely as well as operate the system at room temperature.^[99] However, preparing a single photon source that satisfies all these figures of merit remains an open issue. Relevant reviews can be referred to refs. [22].

Relatively, generating single photons heralded based on parametric sources is still a simple and practical way. A heralded source means the detection of one photon can signal the presence of another due to the correlated emission. The state generated by a parametric nonlinear source can be expressed in photon number or Fock state as

$$|\Psi\rangle = \sum_{n=0}^{\infty} \xi_n |n\rangle_s |n\rangle_i \quad (7)$$

where $|n\rangle$ is photon number state per mode, s and i represent signal and idler respectively. $P_n = |\xi_n|^2$ represents photon number

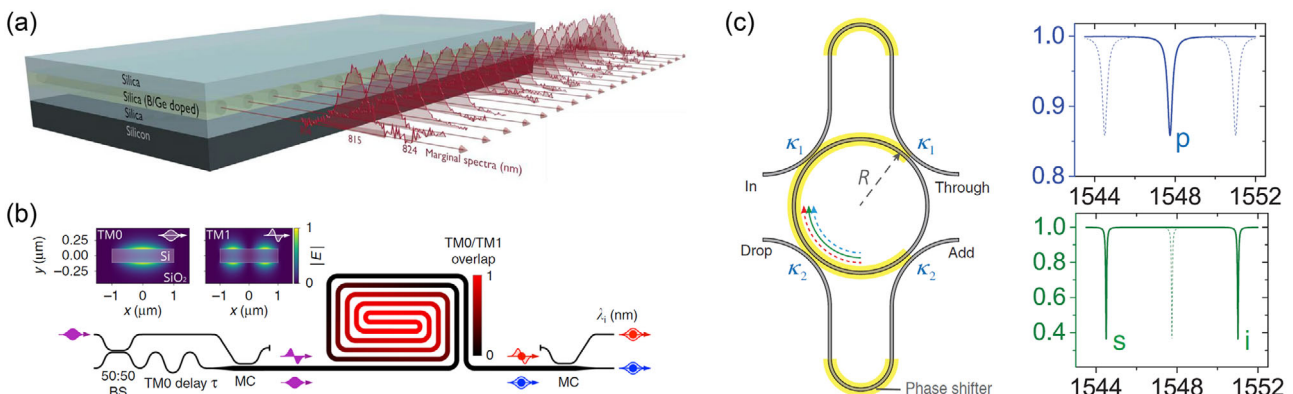


Figure 3. High-purity single photon sources. a) Arrays of near-identical silica-on-silicon heralded single-photon sources. Reproduced with permission.^[117] Copyright 2017, Optical Society of America. b) Intermodal phase-matched silicon waveguide. Reproduced under the terms of a Creative Commons Attribution 4.0 International License.^[116] Copyright 2020, The Authors, published by Springer Nature. c) Dual-AMZI coupled microring. Reproduced with permission.^[78] Copyright 2020, Optical Society of America.

distribution of the source, depending on the pump intensity and material nonlinearity. Ideally, the heralded source should produce one pair of photons deterministically, that is, $P_1 = 1$. In reality, there is always a certain probability of producing vacuum state and multiphoton state. To remove the effects of multi-photon pairs, the pump intensity should be kept low enough, then only the vacuum and single pair states are survived, where the contribution of vacuum state can be eliminated by the heralding process. There is thus a tradeoff between brightness and photon number impurity (multi-photon noise). Obviously, detectors with the ability of resolving photon number are convenient to describe the photon singleness of a source, but they need sophisticated fabrication and operation. In experiments, whether a heralded Fock state indeed contains a single photon can be determined by using a loss-independent Hanbury–Brown and Twiss (HBT) interferometer to measure the second order coherence function ($g^{(2)}(t)$), with $g^{(2)}(0) = 1 - 1/n$ at zero delay for n photons. Whenever $n \geq 1$, $g^{(2)}(0) < 1$, which shows the nonclassical characteristic of light. However, $g^{(2)}(0) < 1$ is not sufficient to indicate single photon emitted, since $n = 2$ corresponds to $g^{(2)}(0) = 0.5$. Thereof a single photon state corresponds to $g^{(2)}(0) < 0.5$.^[100,101] Additionally, the intrinsical probabilistic nature of spontaneous parametric process makes it lack of on-demand characteristics. It has been demonstrated that the optimal heralding efficiency for a single-photon Fock state is no greater than 0.25 by using a single ideal photon pair source and perfect photon number resolving detector.^[102,103] One way to improve the single photon preparation probability is to use multiplexing approach, where the detected heralding signals come from multiple spatial-multiplexed sources or one time- (or frequency-) multiplexed source. Comprehensive reviews about the multiplexing of probabilistic parametric sources can refer to refs. [101, 104].

There is also necessity to obtain high spectral purity for interference-based QIP between single photons. Usually the photon pairs generated by nonlinear parametric processes are correlated, which results in the heralded photon to be projected into a mixed state after the detection of heralding photon. The degree of correlation can be quantified by Schmidt decomposition, where the Schmidt number K represents the effective number of correlated modes.^[101] $K = 1$ (the reciprocal of purity) means the

two-photon state can be factorizable. To achieve this, filters are often used to postselect certain Schmidt modes at the expense of brightness. Solutions to remove the unneeded spectral correlation without the help of lossy filters based on group velocity matching and tailored nonlinearities in SPDC-based crystals and waveguides have been widely investigated,^[105–111] and while experimental realizations of this scheme on CMOS-compatible platform have not yet been demonstrated.

In SFWM-based sources, mode confinement offered by waveguide geometry such as the size and aspect ratio of a rectangular waveguide can be designed to engineer the mode dispersion over a broad near-infrared region as well as the phase matching condition.^[64,85,112–116] By precisely controlling optical modes needed, five near-identical heralded single-photon sources with high-purity have been verified on a laser written silica-on-silicon photonic chip (Figure 3a).^[117] With that, the Hong–Ou–Mandel interference has been generalized to three independent photons. Paesani et al. have achieved a high-quality heralded single photon source through the combination of intermodal SFWM and delayed pump excitation in spiral multimode waveguides.^[116] The design of the multi-modal source is shown in Figure 3b. The pump pulse evolves into two different modes (TM_0 and TM_1) in the structures, and then propagate in the low-loss multimode waveguides with different group velocities. An on-chip TM_0 mode delay line makes the two pump modes largely overlap along the source. By tailoring the cross-section of waveguide, the phase-matching band can be accurately engineered to be similar to the pump bandwidth, leading to frequency uncorrelation. A spectral purity of 0.9904(6) and intrinsic heralding efficiency >0.9 are obtained. The intermodal SFWM, which is dependent on relative group velocities of modes employed, allows the generated photons in discrete narrow bands and thus removes post-filtering.

Although the results of conventional MRR show promise for their utility in generating heralded single photons, their spectral purity is theoretically bounded by 0.93 and one also need to weight the brightness against the heralding efficiency.^[118] At the critical coupling, the heralding efficiency is upper limited to 50%, while in strong over-coupling or under-coupling regime, the efficiency can be close to 1 but with negligible photon

rate.^[118] To circumvent the trade-off, Tison et al. proposed an advanced resonator source embedded in asymmetric MZIs, exhibiting a high coincidence efficiency while without sacrificing the brightness.^[77] Ideally, one would like to have all the input pump circulate in the resonator to generate photon pairs and hence critical coupling condition for pump is needed. On the other hand, it is preferable to extract the signal and idler photons from the resonator immediately after they are generated to minimize the propagation loss in the resonator. Therefore, it is preferable to over-couple the waveguide to the resonator at the wavelength of signal and idler photons. These two conditions can be met simultaneously if the free spectral range of the asymmetric MZIs are designed to be twice that of the ring, so as to suppress every second resonance of the ring, as shown in Figure 3c. By using this structure, a preparation heralding efficiency of 52.4% and spectral purity of 0.95 at relatively low pump power has been realized.^[78] The obtained purity exceeds the theoretical bound 0.93 limited by all the resonances involved have the same linewidth in a single-bus MRR. Another approach for generating spectrally unentangled photon pairs in MRR is to introduce phase shift between two temporally displaced Gaussian pulses,^[75] and a 0.98 spectral purity has been observed experimentally.^[62]

2.1.3. Squeezed Light Source

The standard quantum limit (SQL) usually refers to the minimum level of quantum noise for optical measurement with the use of classical light. In contrast, squeezed light can be used to enhance measurement precision by squeezing the noise in one of the quadratures below the SQL while at the expense of antisqueezing the conjugate quadrature due to the Heisenberg's uncertainty principle.^[119,120] To date, squeezed light has been widely used in sensors,^[121] metrology^[4,122] and continuous variable QIP.^[123,124] Although there are many studies on the generation of squeezed states, most of them are inspired by the following three creative experiments, namely degenerate PDC in $\chi^{(2)}$ materials,^[125] self-phase modulation,^[126] and degenerate FWM^[127] in $\chi^{(3)}$ materials. Recently, much progress has been made in preparing such sources using integrated photonics,^[128–135] especially squeezing light on a CMOS compatible platform due to its scalability and integrability. For example, Dutt et al. directly observed the photocurrent noise squeezing in a Si_3N_4 MRR driven above the parametric oscillation threshold.^[128] Subsequently, tunable squeezing has been realized by varying the coupling between two MRRs.^[129] Squeezed vacuum in a single-mode degenerate configuration has also been proposed based on dual-pump SFWM in MRRs,^[134] where noise contributions from nonparametric effects and unwanted parametric effects can be effectively avoided without significantly sacrificing efficiency.^[135] The breakthroughs for tunable squeezing on a CMOS compatible platform may pay the way for full-chip integrated continuous variable QIP.

2.2. Universal 2×2 Circuit and Phase Shifters

Precise and accurate control of photons has always been the superiority of integrated platforms. On the basis of advanced

COMS technology, more than a thousand active components have been realized in a few mm².^[136] At present, many large-scale quantum photonic experiments are performed using waveguide structures. Most of these circuits are designed for specific applications and can be programmed using software for multiple functions.^[19,23,137–139] In a reconfigurable photonic circuits, photon is controlled by waveguide mesh, whose connectivity determines the possible operations and configurations. Waveguide meshes are mainly formed by a programmable 2×2 circuit, which consists of waveguides, 50:50 power splitter (either multimode interferometers or directional couplers), and phase shifters, as shown in Figure 4a. If all elements are lossless, the circuit corresponds to a SU(2) rotation, and can be described by

$$U = \begin{bmatrix} e^{i\varphi} \sin \frac{\theta}{2} & e^{i\varphi} \cos \frac{\theta}{2} \\ \cos \frac{\theta}{2} & -\sin \frac{\theta}{2} \end{bmatrix}, \quad (8)$$

where θ and φ are the phase shift in the MZI and relative phase between two external arms respectively. This 2×2 circuit is a key building block and it has been demonstrated that any element of the SU(N) ($N > 2$) group can be decomposed into a series of individual SU(2) elements.^[140,141] Practical SU(2) operation suffers from nonidealities due to the imperfect splitting ratio of the couplers, waveguide side-wall roughness and losses associated with phase shifters. Thanks to the development in fabrication technology, less than 0.2 dB loss 2×2 coupler has been reported^[142] and the propagation loss of waveguides can be reduced to 2.7 dB m⁻¹ by minimizing side-wall scattering.^[143] MZI with a 60.5 dB on/off ratio has been demonstrated^[144] without calibrating any components, which is essential to reduce error in quantum operations and thus reduce overhead resources for fault-tolerant linear optical quantum computing.^[145]

Centro-symmetric materials prohibit a $\chi^{(2)}$ natively, phase change often relies on thermo-optic (TO) effect or plasma dispersion (PD) effect. TO modulator, with an integration of electrically driven metallic microheaters above waveguides, has been one of the most widely used reconfiguration devices in nanophotonics. The change in effective refractive index (n_{eff}) with temperature can be written as $\frac{dn}{dT}\Delta T$, where $\frac{dn}{dT}$ is the material's TO coefficient and ΔT represents the temperature change of materials. The TO coefficient of silicon at 300 K near 1550 nm is $1.86 \times 10^{-4} \text{ K}^{-1}$,^[150] about one order of magnitude larger than Si_3N_4 . The TO modulator is easy to use, but each consumes several milliwatts of power, and often produces residual thermal crosstalk between components. To eliminate the crosstalk, Harris et al. used doped resistance and engineered its profile to localize the heat by flowing current perpendicularly to the designed waveguide (Figure 4b).^[146] By employing free-standing strip waveguides, Gao et al. realized the modulation with high efficiency but significant thermal isolation.^[151] The only shortcoming of these TO devices is their slow response time (10–100 μs) due to the slow heat diffusion process, which can be an obstacle in many quick-responded signal processing applications. For example, the rapid change of the optical properties is important for performing the feed-forward operation in generating heralded single photon and linear optical quantum computing or teleportation. PD modulators based on fast injection or depletion of carriers, are appealing due to the CMOS compatibility and speeds of tens of gigahertz

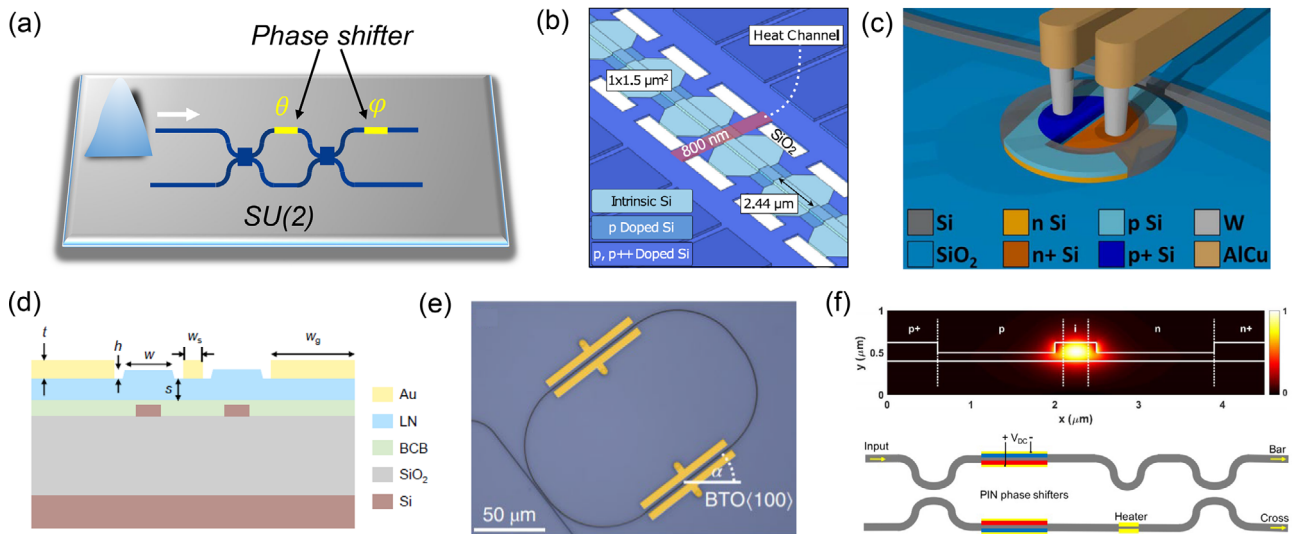


Figure 4. a) Universal 2x2 circuit. b) Engineered resistance profile on dopant silicon. Reproduced with permission.^[146] Copyright 2014, Optical Society of America. c) Scanning electron microscope image of the micro-disk modulator composed of a silicon disk with a diameter of 3.5 μm and a coupled strip waveguide. Reproduced with permission.^[147] Copyright 2017, Optical Society of America. d) Hybrid integration of thin film lithium niobate modulator on silicon. Reproduced with permission.^[30] Copyright 2019, Springer Nature. e) Hybrid integration of barium titanate modulator. Reproduced with permission.^[148] Copyright 2019, Springer Nature. f) Integrated PIN junction modulator. The p and n (p+ and n+) regions were formed by boron difluoride and arsenic implants (boron difluoride and phosphorus implants). Reproduced with permission.^[149] Copyright 2020, Optical Society of America.

(GHz).^[152] It has also been investigated at cryogenic temperatures (Figure 4c).^[147] However, the change of carriers concentration can cause a change in absorption and losses.

Pockels-effect-based electro-optic modulators, which are, in principle, not limited by operation conditions. Integrating materials possessing a strong Pockels effect with silicon is a promising way for multi-functional integrated quantum devices. Hybrid integration techniques have been used to integrate lithium niobate (Figure 4d)^[30] and barium titanate^[153] on silicon, achieving tens of GHz speed with low loss. It is shown that the Pockels coefficient of barium titanate at cryogenic temperature can be maintained at 200 pm V⁻¹ (Figure 4e).^[148] Recently, DC-Kerr-effect-based modulator operated at a temperature of 5 K with GHz speeds has also been demonstrated by producing an effective electric-field-induced $\chi^{(2)}$ is silicon (Figure 4f),^[149] which can be explored as a pathway for emerging cryogenic quantum applications.

2.3. Single Photon Detector

The integration of optical components including sources, modulators and detectors is a necessary requirement for the advancement of photonic chip. Within such assemblies, special requirements are put forward for detectors to possess unity detection efficiency, zero dark counts, no dead time, and perfect time resolution. However, realistic detectors can only approach these particular features due to inherent limitations of the detection mechanism. Among the various single-photon detection devices, such as photo-multiplier tubes, single-photon avalanche diodes, superconducting detectors are widely used, among them SNSPDs are the most attractive devices. SNSPDs have the advantages of excellent detection efficiency, high signal-to-noise

ratio, fast recovery time, and low time jitter, providing prominent ability for detecting broadband weak light. The remarkable properties of SNSPDs are beneficial for both quantum and classical applications, from quantum computation, secure communication, and metrology to classical faint light applications.

SNSPD works by maintaining the superconducting material well below its critical temperature and biasing the current close to its critical current. Even if only one photon hits, the energy is enough to transit the nanowire from superconducting state to normal state, and generate a voltage pulse subsequently. The voltage pulse is further filtered and amplified, and discriminated as a photon detection event.^[154,155] A range of superconducting materials have been developed for SNSPD on silicon substrate, including niobium nitride,^[156,157] niobium-titanium-nitride,^[158,159] tungsten silicide,^[160] and molybdenum silicide,^[161] boosting hybrid integration with reconfigurable photonic circuits,^[159,162] which not only bridge different high-quality building blocks, but also enable configurable linear optical operations required by QIP. Recent experimental work on molybdenum silicide SNSPD has shown >98% detection efficiency at a wavelength of 1550 nm by optimizing the design and fabrication of an all-dielectric layered stack and fiber coupling package.^[163] Additionally, SNSPD outperform other detectors in terms of ultralow (480 ps) recovery time,^[164] record-high time resolution (<3 ps),^[165] and low dark count rate.^[166] In some applications, such as imaging and heralding single-photon sources, SNSPD with a large number of pixels and photon number resolution (PNR) capability are needed. Wollman et al. have reported a 32 × 32-pixel SNSPD array using row-column readout architecture.^[167] However, the integration of multiple high-efficiency SNSPDs on a single chip is challenging due to the material lattice mismatch, which can lead to low yield. It is possible to post-integrate only high-performance SNSPDs using the pick-and-place technique,^[157]

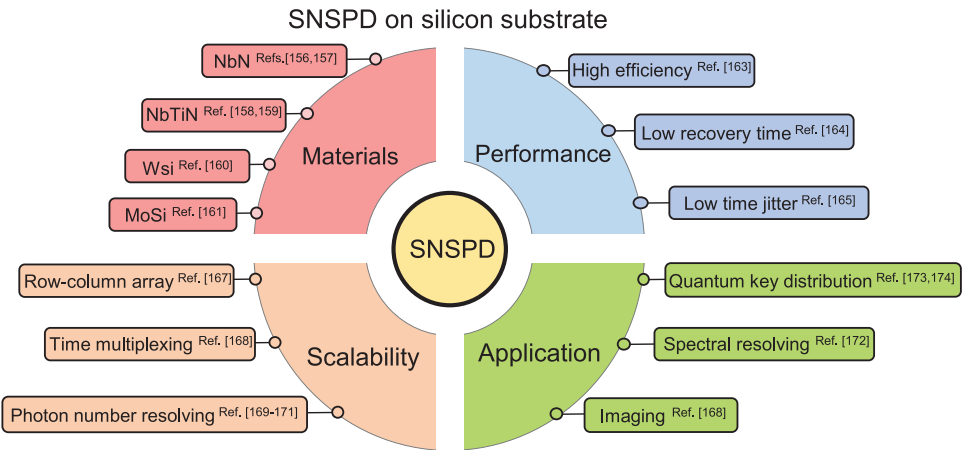


Figure 5. Overviews of SNSPD on silicon substrate. It summarizes four aspects and lists main progress in this field.

where each SNSPD is evaluated individually before being integrated. Time-multiplexing scheme can be used to realize single photon imager and simplify device design and fabrication.^[168] In this scheme, the SNSPD is not only a single-photon detector but also an efficient microwave delay line, enabling the readout of the position and time of photon-absorption events from the arrival times of the detection pulses. Going forward, the strong limit of SNSPDs is the lack of full PNR capabilities. To this end, amplitude multiplexing scheme^[169] and impedance technique^[170] for SNSPDs have been developed without increasing the heatload of cryogenic system. Resolution up to 4 photons with 16.1 ps timing jitter is achieved.^[171] More recently, the integration of on-chip spectrometers has been demonstrated,^[172] covering wavelengths range from 600 to 2000 nm, which can be useful for astronomical observation, spectroscopic imaging and wavelength division multiplexed quantum communications. Heterogeneous superconducting-photonic chips in quantum communication have also been reported,^[173,174] benefiting low-cost and scalable applications.

3. The Application of Integrated Quantum Photonics

Quantum-enhanced technologies promise extreme advantages over ordinary classical means. While several physical systems have been investigated, photonic quantum technologies have raced ahead thanks to the relative simplicity in the generation, manipulation, and detection. Compared with other platforms, a great advantage of photon is that it can naturally be encoded in various DOFs, including orbital angular momentum,^[175,176] frequency,^[63,89] path,^[37,177] and temporal.^[178,179] Moreover, several DOFs of one photon can be used simultaneously.^[90] The ability to implement quantum technologies on photonic chips or circuits is essential for making quantum technologies from the laboratory to real world.

The natural scheme of quantum state encoding for a single photon on chip is in a superposition of waveguide paths. Photons simultaneously locate at two/multiple waveguide paths

form quNit ($N \geq 2$). Recent advances in fabrication techniques can highly integrate waveguides, beam splitters and phase shifters on a single chip,^[20] allowing quNit operation with high quality.^[37,66,79] Two qubit operation needs to be able to apply conditional operation to one qubit according to the state of the other one. Compared with the single qubit operation, it is difficult to realize this operation, because it is a kind of nonlinear optical interaction, which is quite weak at the single photon level. Another option is to use linear optics and measurements to mimic nonlinear operation, resulting in a probabilistic gate after appropriate post selection^[180] or additional heralding signals.^[137,181] In this section we will introduce the state of the art work of photonic QIP.

3.1. Programmable Quantum Photonic Processor

Integrated quantum photonic processors (QPPs) are particularly attractive for their high interferometric visibilities, phase stability, low loss, and powerful scalability to many passive and active components.^[19,23,137,182] The majority of universal unitary transformation have been designed based on the scalable schemes proposed by Reck et al.^[183] and Clements et al.,^[141] respectively. Figure 6 gives an example of the realization of four modes unitary transformation composed of six SU(2) modules. Studies have shown that even if all individual components have fabrication defects, high-fidelity operation remains possible in large-scale QPP.^[184–186] To date, large-scale quantum photonic circuits have been realized, as the fabrication processes have been well-studied and ensure the preparation of reconfigurable, high-quality photonic chips.^[19,23,187–190] For example, a waveguide mesh including 88 MZIs and 176 individually tunable TO phase sifters has been used to model quantum particle transport, where lattice sites are represented as the waveguides (Figure 6b).^[187] These components are sufficient to construct arbitrary unitary transformation of U(9). External phase shifters (φ in Equation (7)) of the sub-units U(2) were set to study both the static and dynamic disorder separately and simultaneously. Distinct transport regimes have

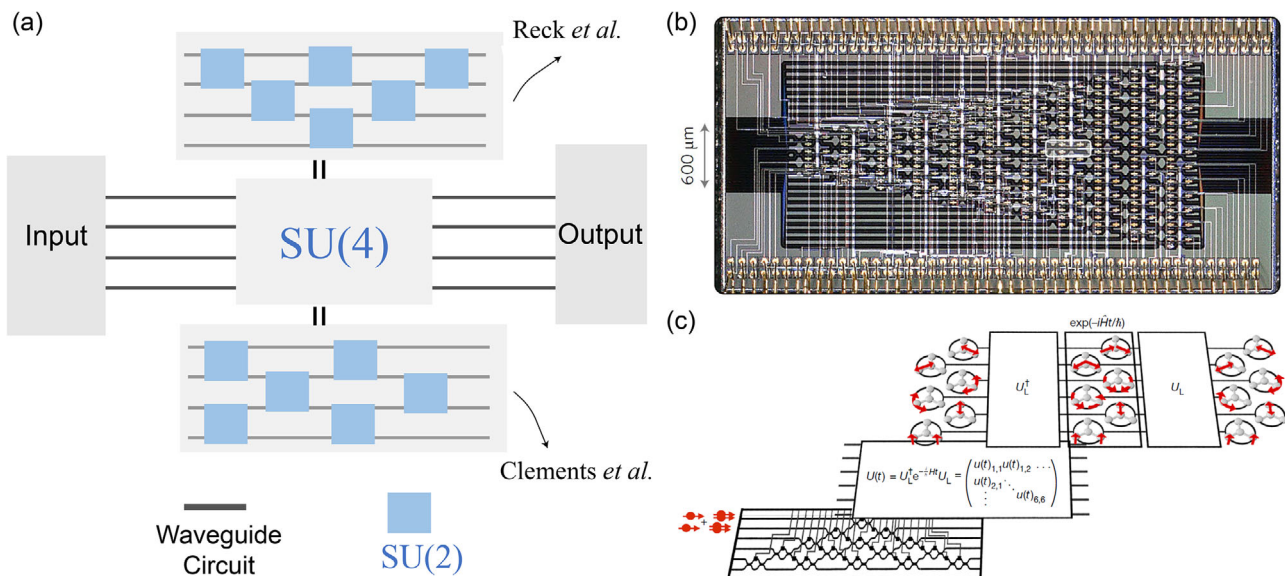


Figure 6. a) Programmable photonic processor for universal four modes unitary transformation composed of six SU(2) modules. Up (down) shows a scheme designed by Reck et al.^[183] (Clements et al.^[141]). b) Optical micrographs of large-scale programmable QPP on silicon. Reproduced with permission.^[187] Copyright 2017, Springer Nature. c) Quantum simulation for the vibrational dynamics of molecules with a linear optical circuitry. Reproduced with permission.^[191] Copyright 2018, Springer Nature.

been observed over 64 400 experiments, benefiting from low-loss and the high-fidelity programmable transformations. The device has also been used to demonstrate variational quantum unsampling protocol, which is a nonlinear quantum neural network approach used to verify and infer the outputs of near-term quantum circuits.^[190] In this protocol, one can train a quantum operation layer-by-layer to acquire the effect of the unknown unitary state on the known input state, that is learning the inverse of the black-box quantum dynamics. Moreover, quantum dynamic behaviour in several molecules has been simulated on a programmable photonic chip consists of an array of six germanium doped silica cores^[191] (Figure 6c). According to the direct mapping between quantum systems and photonic quantum technologies, the full space of vibrational dynamics for a general molecule composed of up to four atoms can be explored by the six-mode simulator. Scaling up the techniques may power the field of femtochemistry in the nearer term.

3.2. Multi-Dimensional Quantum Information Processing

Multi-dimensional entangled states have attracted much attention because of their unique properties. For instance, qudits can provide higher channel capacity and tolerant more noise in quantum communication,^[192–195] as well as enable higher efficiency and robustness in quantum computing^[66,196,197] and simulations.^[198] From a basic point of view, qudits also provide high degree of violating generalized Bell inequalities,^[199] lower bounds on Bell tests with no fair-sampling loopholes^[199] and capabilities of revealing quantum contextuality.^[200] Particularly, path-entangled photon pairs are attractive because of their simplicity in concept and have been extensively investigated in the field of QIP.^[183] However, to generate high-quality path-

entangled photon pairs usually requires to coherently pump several indistinguishable photon-pair source simultaneously and highly stabilize the phase of multi-path interferometers.^[201] With the increase of dimension, the long term phase stabilization becomes an arduous task in experiments based on discrete optical components.

Recent developments of on-chip high-dimensional entanglement has indicated silicon as a leading platform for large-scale QIP.^[37,66,72,79,202] Silverstone et al.^[203] used a silicon chip including MRR sources, demultiplexers and reconfigurable 2×2 circuits to generate path-entangled two-qubit state (Figure 7a). Such fully integrated photon-pair source has formed a primitive system of quantum photonic chips and promoted many impressive applications, such as finding eigenstates of a Hamiltonian by combining variational methods and phase estimation with >99% fidelity,^[204] learning the Hamiltonian of an electron spin in a diamond nitrogen-vacancy center via Bayesian interference,^[205] and implementing Bayesian phase estimation algorithm and using the algorithm to simulate hydrogen molecular energies.^[206] Lu et al. employed dual-MZI MRR sources, demultiplexers, and multi-port interferometers to generate, manipulate and detect path-entangled qutrits ($N = 3$) (Figure 7b).^[79] By virtue of the generated two-qutrit entangled state, they simulated a graph composed of two vertex and three edges and counted the perfect matching in this graph, which is a #P hard problem.^[207,208] It can be regarded as the first step toward solving #P complex problems with quantum photonic devices. They also demonstrated the excellent phase sensitivity of qutrit-entangled system, exceeding the limit of both classical three-path linear interferometer and quantum second-order nonlinear interferometer. Qiang et al. constructed two pre-entangled ququarts ($N = 4$) and probabilistically realized 98 different two-qubit unitary operations with an average fidelity of 93% via Hilbert-space-expansion approach^[66] (Figure 7c).

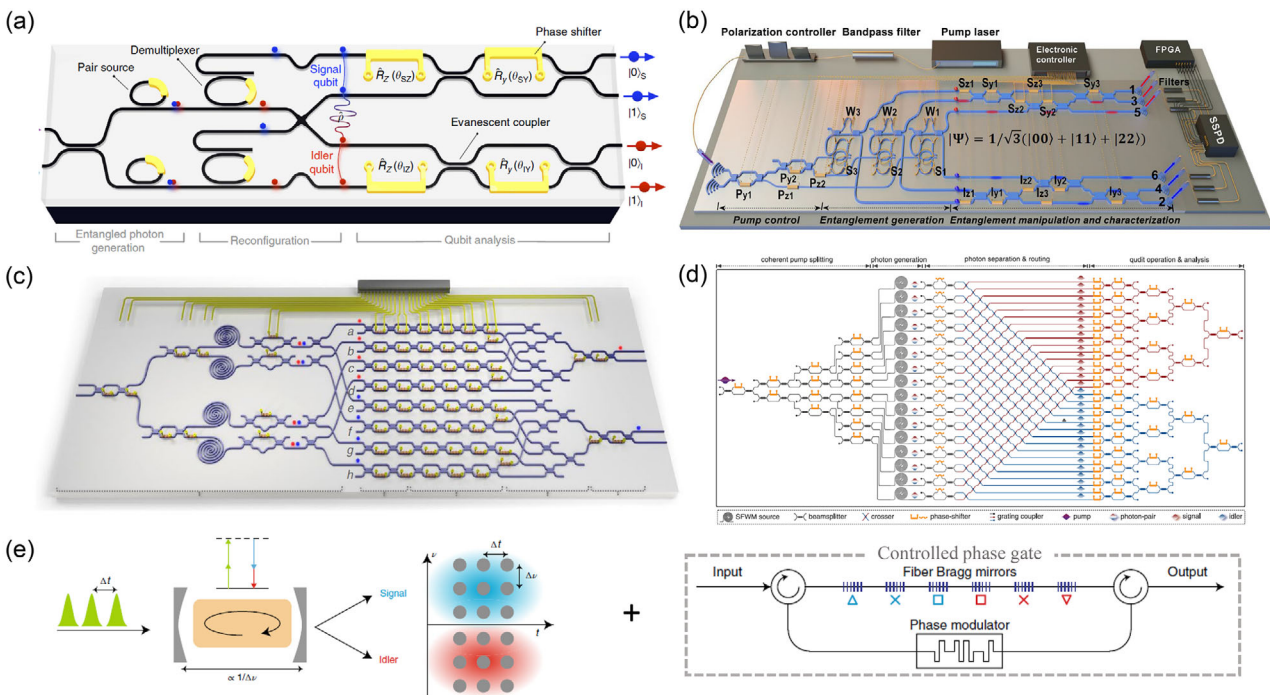


Figure 7. Diagrams of the devices for the chip-scale two-photon entanglement generation and manipulation in multidimensions. a) 2D. Reproduced under the terms of a Creative Commons Attribution 4.0 International License.^[203] Copyright 2015, The Authors, published by Springer Nature. b) 3D. Reproduced under the terms of a Creative Commons Attribution 4.0 International License.^[79] Copyright 2020, The Authors, published by Springer Nature. c) 4D. Reproduced with permission.^[66] Copyright 2018, Springer Nature. d) 15D. Reproduced with permission.^[37] Copyright 2018, American Association for the Advancement of Science (AAAS). e) High dimension in both the frequency and time domains. Reproduced with permission.^[90] Copyright 2019, Springer Nature. In (a)-(d) experiments, the entanglement is generated by coherently exciting several sources with two pump photons annihilated and one pair of signal and idler photons created. The generated photons are separated by spectral demultiplexers and manipulated by reconfigurable circuits. Finally, the photons are collected and detected by single photon detectors at the outputs. In (e), the photon pairs in three frequency modes are produced by pumping the MRR-based micro-comb source with three phase-locked pulses. A controlled phase gate is used to transform the hyperentanglement state to three-level, four-partite cluster states.

Different from the circuit model of quantum computing, arbitrary unitary operation of any two qubits is realized by the linear combination of four unitaries, which are easy to implement in the scheme. Each unitary is the tensor product of two single qubit unitaries.^[209] They exhibited the performance of the quantum processor by implementing the quantum approximate optimization algorithm for finding solutions to constraint satisfaction problems, and simulating Szegedy quantum walks on a two-node four-weight graph. More powerfully, Wang et al. realized a programmable bipartite entangled state with dimensions up to 15×15 (Figure 7d).^[37] The device integrated more than 550 components on an individual quantum photonic chip. Several previously unexplored high-dimensional quantum applications, such as certifying multidimensional quantum randomness expansion and entangled state self-testing, have been investigated. These high-quality functionalities including on-chip generation, manipulation, and analysis of multidimensional quantum systems, demonstrated the capabilities of large-scale QIP with silicon.

Hyperentanglement, meaning a quantum system that can be entangled in multiple DOF simultaneously, is also an important resource in QIP due to its large Hilbert space and advantages in deterministic Bell state analysis.^[210] Reimer et al. generated a three-level, four-partite cluster state based on a Hydex chip by a transformation of high dimensional hyperentangled state in time

and frequency domains.^[90] The transformation is carried out by the controlled phase gate as shown in Figure 7e. The generated d-level cluster states provided better noise tolerance than conventional two-level cluster states, and beneficial for high dimensional one-way QIP.

3.3. Multi-Photon Quantum Information Processing

The power of a quantum device is closely related to Hilbert space it can access. The Hilbert space spanned by quantum states can be expressed as d^n , where d is the dimensions of a particle and n is the number of particles in the states. Increasing the dimensions or modes of a photon can only polynomially scale the Hilbert space. Thus, to build a scalable quantum device, the use of multi-photon sources is indispensable for exponential space scaling. Only recently has on-chip quantum interference with heralded photons from two independent MRRs been demonstrated,^[211] implying the feasibility of integrated multi-photon QIP. Subsequently, several on-chip multi-photon technologies have been demonstrated.^[38,69,70,212] Various types of four-photon four-qubit graph states have been generated on a mass-manufactured chip by postselecting a reconfigurable entangling gate (Figure 8a).^[69] The gate can be programmed

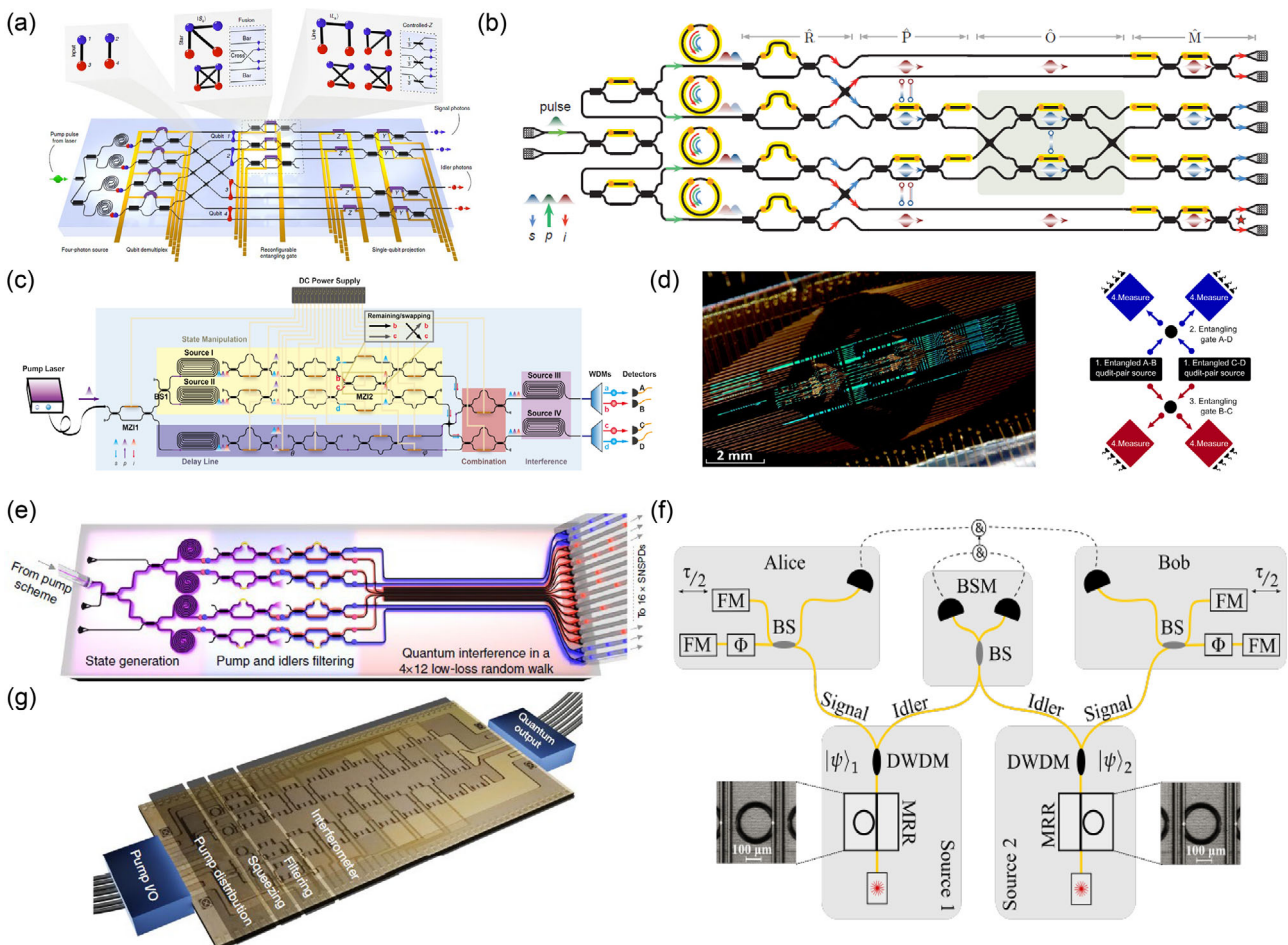


Figure 8. Chip-scale quantum information processing with multi-photon. a) Schematic lay out of the device for generating four photons graph state by combining two postselected Bell-pairs in reconfigurable gates. Reproduced under the terms of a Creative Commons Attribution 4.0 International License.^[69] Copyright 2019, The Authors, published by Springer Nature. b) On-chip genuine multipartite entanglement and quantum teleportation in silicon. Reproduced with permission.^[212] Copyright 2020, Springer Nature. Two pairs of nondegenerate photons are generated in an array of four MRR sources and manipulated by linear-optics multi-qubit entangling circuits. c) Experimental setup to observe frustrated four-photon interference on a silicon photonic chip. Reproduced with permission.^[216] Copyright 2021, The Authors. d) Photograph of the silicon photonic chip and schematics of the modules for realizing eight-qubit reconfigurable graph states by four photons. Reproduced with permission.^[70] Copyright 2021, published by Springer Nature. e) Boson sampling with up to eight photons on a silicon chip. Reproduced with permission.^[38] Copyright 2019, Springer Nature. f) Continuous wave pumped entanglement swapping between two independent MRRs based on Si_3N_4 integrated platform. Reproduced under the terms of Creative Commons Attribution CC-BY license.^[88] Copyright 2021, The Authors, published by IOP Publishing. g) Squeezing-based programmable photonic chip for proof-of-principle demonstrations of quantum algorithms. The nanophotonic device contains modules for generating squeezed states, filtering pump noise and implementing linear optical transformation on subspaces of the squeeze light. Reproduced with permission.^[25] Copyright 2021, Springer Nature.

to perform either a fusion or controlled-Z operation for the generation of star- or line-type entanglement respectively. Graph states are important building blocks of large-scale quantum technology. Among them, the cluster state is a key resource in one-way computing and may be more promising to realize universal quantum computing than gate-based models. The failure of using nondeterministic fusion operations to build a larger cluster state has no influence on the initial entangled states.^[213] In ref. [69], the count rates obtained are comparable to those observed in the first multi-photon experiments,^[214] and the authors explained that four-photon rates could be propelled to 100-kHz regime with state-of-the-art technologies. Llewellyn et al. employed four MRR sources and linear-optics multi-qubit

entangling circuits demonstrating genuine on-chip multipartite entanglement and quantum teleportation in silicon with high fidelity (Figure 8b).^[212] The multiple MRR sources are locked within a few pm for long integration time and approaching optimal levels of purity, indistinguishability, and heralding efficiency. Even better, simultaneously scaling up the number of photons and the dimensionality would further enlarge the Hilbert spaces, which is a great advantage of photons.^[215] Different from adopting interference of different intrinsic properties of particles, ref. [216] demonstrated the multi-partite generalization of frustrated down conservation (Figure 8c), which was proposed via a detour to graph theory.^[208] In that way, the birthplaces of the four photons are in a coherent superposition and one can observe

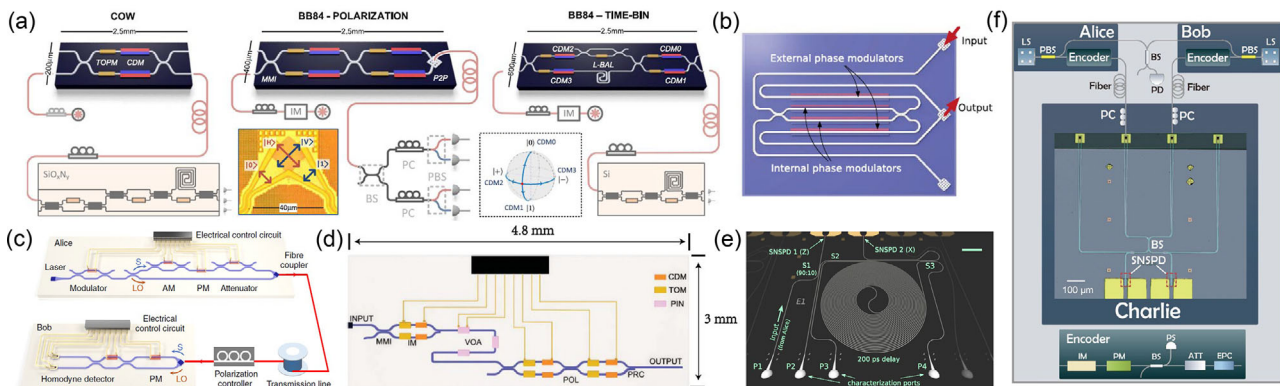


Figure 9. Silicon based quantum key distribution. a) Silicon photonics devices for coherent-one-way, polarization encoded and time-bin encoded QKD. Reproduced with permission.^[40] Copyright 2017, Optical Society of America. b) Metropolitan QKD with silicon photonics. Polarization grating couplers are employed to convert between polarization and path DOF. Reproduced under the terms of a Creative Commons Attribution 4.0 International License.^[235] Copyright 2018, The Authors, published by American Physical Society. c) Schematic of chip-based continuous variable QKD system. Reproduced with permission.^[41] Copyright 2019, Springer Nature. d) Transmitters integrated polarization-encoding MDI-QKD chip, manufactured by standard silicon photonics platform and packaged for the purpose of commercial production. Reproduced under the terms of a Creative Commons Attribution 4.0 International License.^[42] Copyright 2020, The Authors, published by American Physical Society. e) Receiver chip for different time-based QKD protocols, including photonic circuitry and waveguide-integrated SNSPDs on a single Si_3N_4 chip. Reproduced under the terms of a Creative Commons Attribution 4.0 International License.^[173] Copyright 2021, The Authors, published by Springer Nature. f) Schematic of MDI-QKD experimental setup with an integrated heterogeneous superconducting-silicon-photonics platform. Reproduced with permission.^[174] Copyright 2019, The Authors.

constructive or destructive interference of four-photon systems that cannot be observed in the photon pairs themselves.

Encoding multiple qubits onto single photons in a multi-photon state can efficiently save quantum computing resource. Accordingly, Vigliar et al. produced error-protected qubits and compared several schemes with and without error-correction encodings with reconfigurable graph states (Figure 8d).^[70] With error protection, the success rate can be increased from 62.5% to 95.8% when running a phase estimation algorithm. It was conjectured that the resource savings of high-dimensional encodings can develop with up to ≥ 40 qubits, approaching a scale impractical with previous pre-loss-tolerant photonic schemes. In parallel, many multi-photon experiments in the path DOF,^[1,38,217–220] have recently been motivated by the boson sampling proposal,^[221] which could unveil the quantum computational advantage over classical computing. Boson sampling is a computational problem that when a linear optical circuits (composed of arrays of beam splitters and phase-shifters) act on multiple input indistinguishable photons generate an output probability distribution that cannot be efficiently solved classically. By now, up to eight photons sampling over 12 waveguides has been reported in a single chip^[38] (Figure 8e). Using degenerate or nondegenerate SFWM, Paesani et al. generated the squeezed state or Fock state, switching between scatter shot and Gaussian boson sampling. They also benchmarked the algorithm for calculating molecular vibronic spectra.^[222]

Meanwhile, the Si_3N_4 based integrated platform has also attracted significant attention in multi-photon QIP very recently.^[25,88] Using state-of-the-art time-resolved detector, Samara et al. obtained an entanglement swapping visibility over 0.91 with two independent Si_3N_4 MRRs in the continuous wave regime (Figure 8f).^[88] By making the uncertainty in detection time smaller than the photons' coherence time, the synchronization for entanglement distribution between distant locations

can be simplified. For near-term demonstrations of quantum computational advantage, a full-stack hardware software system is introduced on a programmable Si_3N_4 chip (Figure 8g).^[25] Such squeezing-based photonic machines with high sampling rate have been used to carry out three quantum algorithms, that is, Gaussian boson sampling, molecular vibronic spectra and graph similarity, showcasing the capabilities of the nanophotonic chip. Although the device at present can be reached by a classical computer, the programmability and scalability enable such platform to perform bosonic quantum algorithms in a large scale.

3.4. Integrated Quantum Key Distribution

QKD can offer theoretical security in the framework of quantum mechanics.^[3,223–225] Various DOFs of photons have been employed in QKD,^[226] depending on the application scenarios. After decades of development, the theory and techniques of QKD are relatively mature, and have been extended to large-scale quantum network over 4600 km.^[9] From the perspectives of technologies, metropolitan QKD can leverage the existing optical fiber networks and high-speed photonic interconnect architectures developed for classical telecommunications. As such, most of the research on integrated QKD focuses on sources, modulators and circuits that are mature in CMOS foundry services. The photonic integration techniques provide a compact and stable avenue for the integration of both photonic and electronic components monolithically.^[227] They also allow experimentalists to design quantum devices on different platforms to meet all kinds of the stringent requirements of QKD devices.^[21,22,46]

In recent years, there have been several demonstrations on integrated quantum communication.^[39–42,174,228–241] Remarkably, Sibson et al. operated three QKD protocols at a speed of GHz with standard silicon photon fabrication (Figure 9a).^[40] Phase-

dependent loss in carrier-depletion modulators is minimized by using slow TO phase modulators to bias the circuits with high-fidelity states prepared. Field tests of high-speed polarization-based QKD have been demonstrated by using integrated MZI modulator encoder (Figure 9b).^[235] Polarization grating couplers are employed to convert path encoding on the chip to polarization in the fibers, with more than 25 dB polarization extinction ratio. An integrated silicon photonic chip has been exploited for Gaussian-modulated continuous variable QKD (Figure 9c).^[41] With all components except laser, that is, modulators, multiplexers and homodyne detectors, are integrated on a single photonic chip packaged with a printed circuit board.

Despite the tremendous progress in QKD, practical implementations still deviate from the theoretical description in security proofs, which may open side-channel attacks.^[242–245] For example, a series of loopholes have been observed due to imperfections of measurement devices.^[225] To avoid all detector side attacks, measurement-device-independent QKD (MDI-QKD) has been proposed.^[246,247] Different from traditional trusted-nodes-based QKD protocols, it requires the untrusted central (Charlie) to perform Bell state measurement and creates correlations between senders from postselected coincidence events. The outstanding features of MDI-QKD have attracted many experimental demonstrations with standard, off-the-shelf components.^[176,248–255] Furthermore, the topology of MDI-QKD is similar to that of star-like quantum networks and can seamlessly integrate to the metropolitan networks.^[256–258] By now, transmitters-integrated MDI-QKD has been experimentally realized with time-bin and polarization encoding.^[42,237] For example, ref. [42] demonstrated a 1.25 GHz on-chip MDI-QKD transmitting using polarization encoding and achieved excellent secret rate of 31 bit/s even over 36 dB channel loss (Figure 9d). The size of the packaged chip is 20×11×5 mm³ and is easy to assemble by using commercial foundry. Full chip integrated MDI-QKD system except lasers and detectors has subsequently been implemented on silicon.^[241] These breakthroughs provide a scalable, portable, stable, and miniaturized solution for MDI-QKD transmitter.

Single-photon detectors as unique and quintessential devices for QKD, have also been integrated on a chip and applied to QKD recently (Figure 9e).^[173] The receiver, including SNSPDs and components needed for different time-based QKD protocols is fabricated on a low-loss Si₃N₄ chip. Zhang et al. reported the realization of waveguide integrated SNSPDs on a heterogeneous superconducting-silicon chip and the application of it in a time-bin encoded MDI-QKD experiment (Figure 9f).^[174] By measuring the coincidence counts between two different detectors at different time bins, they projected the two photons onto the singlet state, $|\Psi^-\rangle = 1/\sqrt{2}(|el\rangle - |le\rangle)$, where |e⟩ and |l⟩ stand for the quantum states of photons being early (e) or late (l).

4. Summary and Outlook

In this review, we have presented recent advances in integrated quantum photonic systems used to generate, manipulate and efficiently detect the state of photons. Chip-based sources are widely studied for generating single photons, entangled-photon pairs and squeezed states with high efficiency. Programmable

photonic circuits with low optical insertion loss and low electrical power consumption phase shifters have been demonstrated in silicon photonics, making this platform appealing for quantum application. Recent approaches for the heterogeneous integration of superconducting materials with photonic circuits may provide a solution for the long-standing issue of fully integrated quantum chips. Also, existing large-scale experiments on silicon substrate have solidified it as a valuable platform for future quantum technologies.

Despite these progress, the realization of practical system-level quantum photonic devices with high-quality building blocks still facing many challenges. One major obstacle is all the components need to run in a common environment. Since SNSPD needs low temperature to guarantee its high performance, a low-temperature-compatible phase tuning schemes is required, such as electro-optic, opto-mechanical,^[159] or DC-Kerr effects, to develop a low-loss and programmable cryogenic photonic circuitry. Another challenge is realizing deterministic two-qubit operation which could take photonic QIP to a distinctive direction. It is hard to satisfy, because such nonlinear interaction at single photon level is extremely weak. Although the proposal of nonclassical interference^[14] allow the realization in a heralding way, it needs a lot of auxiliary qubits and classical feed-forward. Moreover, on a more practical side, classical interface hardware for an integrated quantum system is mostly realized by discrete electronics that limit the practicability of devices.^[227] High-performance classical data acquisition and processing system need to be scaled up with underpinning quantum hardware.^[25] Therefore, fully exploiting the integration of silicon quantum photonics with CMOS microelectronic is of particular importance. Although it remains technologically difficult to build full stack integration of quantum photonic devices, the field of integrated quantum photonics is vigorously developing and pointing to a bright future for quantum applications.

Acknowledgements

This research is supported by the National Key Research and Development Program of China (2017YFA0303700), National Natural Science Foundation of China (Grant No. 11674170, 11621091, 11321063, 11804153), NSFC-BRICS (No. 61961146001), NSF Jiangsu Province (No. BK20170010), the program for Innovative Talents and Entrepreneur in Jiangsu, and the Fundamental Research Funds for the Central Universities.

Conflict of Interest

The authors declare no conflict of interest.

Keywords

quantum information processing, quantum communication, quantum optics, silicon photonics

Received: May 20, 2021

Revised: August 16, 2021

Published online: November 9, 2021

- [1] T. D. Ladd, F. Jelezko, R. Laflamme, Y. Nakamura, C. Monroe, J. L. O'Brien, *Nature* **2010**, 464, 45.

- [2] N. Gisin, G. Ribordy, W. Tittel, H. Zbinden, *Rev. Mod. Phys.* **2002**, *74*, 145.
- [3] V. Giovannetti, S. Lloyd, L. Maccone, *Nat. Photonics* **2011**, *5*, 222.
- [4] H.-S. Zhong, H. Wang, Y.-H. Deng, M.-C. Chen, L.-C. Peng, Y.-H. Luo, J. Qin, D. Wu, X. Ding, Y. Hu, P. Hu, X.-Y. Yang, W.-J. Zhang, H. Li, Y. Li, X. Jiang, L. Gan, G. Yang, L. You, Z. Wang, L. Li, N.-L. Liu, C.-Y. Lu, J.-W. Pan, *Science* **2020**, *370*, 1460.
- [5] A. Bouland, B. Fefferman, C. Nirke, U. Vazirani, *Nat. Phys.* **2019**, *15*, 159.
- [6] F. Arute, K. Arya, R. Babbush, D. Bacon, J. C. Bardin, R. Barends, R. Biswas, S. Boixo, F. G. Brandao, D. A. Buell, B. Burkett, Y. Chen, Z. Chen, B. Chiaro, R. Collins, W. Courtney, A. Dunsworth, E. Farhi, B. Foxen, A. Fowler, C. Gidney, M. Giustina, R. Graff, K. Guerin, S. Habegger, M. P. Harrigan, M. J. Hartmann, A. Ho, M. Hoffmann, T. Huang, et al., *Nature* **2019**, *574*, 505.
- [7] C. S. Hamilton, R. Kruse, L. Sansoni, S. Barkhofen, C. Silberhorn, I. Jex, *Phys. Rev. Lett.* **2017**, *119*, 170501.
- [8] S.-K. Liao, W.-Q. Cai, W.-Y. Liu, L. Zhang, Y. Li, J.-G. Ren, J. Yin, Q. Shen, Y. Cao, Z.-P. Li, F.-Z. Li, X.-W. Chen, L.-H. Sun, J.-J. Jia, J.-C. Wu, X.-J. Jiang, J.-F. Wang, Y.-M. Huang, Q. Wang, Y.-L. Zhou, L. Deng, T. Xi, L. Ma, T. Hu, Q. Zhang, Y.-A. Chen, N.-L. Liu, X.-B. Wang, Z.-C. Zhu, C.-Y. Lu, et al., *Nature* **2017**, *549*, 43.
- [9] Y. Chen, Q. Zhang, T. Chen, W. Cai, S. Liao, J. Zhang, K. Chen, J. Yin, J. Ren, Z. Chen, S. Han, Q. Yu, K. Liang, F. Zhou, X. Yuan, M. Zhao, T. Wang, X. Jiang, W. Liu, Y. Li, Q. Shen, Y. Cao, C. Lu, R. Shu, J. Wang, L. Li, N. Liu, F. Xu, X. Wang, C. Peng, J. Pan, *Nature* **2021**, *589*, 214.
- [10] N. Peters, J. Altepeter, E. Jeffrey, D. Branning, P. Kwiat, *J. Quantum Inf. Comput.* **2003**, *3*, 503.
- [11] A. Yimsiriwattana, S. J. Lomonaco Jr, in *Quantum Information and Computation II*, Proc. SPIE Vol. 5436, SPIE, Bellingham, WA **2004**, pp. 360–372.
- [12] S. Barz, E. Kashefi, A. Broadbent, J. F. Fitzsimons, A. Zeilinger, P. Walther, *Science* **2012**, *335*, 303.
- [13] N. Gisin, R. Thew, *Nat. Photonics* **2007**, *1*, 165.
- [14] E. Knill, R. Laflamme, G. J. Milburn, *Nature* **2001**, *409*, 46.
- [15] R. Raussendorf, D. E. Browne, H. J. Briegel, *Phys. Rev. A* **2003**, *68*, 022312.
- [16] M. A. Nielsen, *Phys. Rev. Lett.* **2004**, *93*, 040503.
- [17] M. Gimeno-Segovia, P. Shadbolt, D. E. Browne, T. Rudolph, *Phys. Rev. Lett.* **2015**, *115*, 020502.
- [18] R. Raussendorf, H. J. Briegel, *Phys. Rev. Lett.* **2001**, *86*, 5188.
- [19] N. C. Harris, J. Carolan, D. Bunandar, M. Prabhu, M. Hochberg, T. Baehr-Jones, M. L. Fanto, A. M. Smith, C. C. Tison, P. M. Alsing, D. Englund, *Optica* **2018**, *5*, 1623.
- [20] J. Wang, F. Sciarrino, A. Laing, M. G. Thompson, *Nat. Photonics* **2020**, *14*, 273.
- [21] A. W. Elshaari, W. Pernice, K. Srinivasan, O. Benson, V. Zwiller, *Nat. Photonics* **2020**, *14*, 285.
- [22] J.-H. Kim, S. Aghaeimeibodi, J. Carolan, D. Englund, E. Waks, *Optica* **2020**, *7*, 291.
- [23] W. Bogaerts, D. Pérez, J. Capmany, D. A. Miller, J. Poon, D. Englund, F. Morichetti, A. Melloni, *Nature* **2020**, *586*, 207.
- [24] X. Qiang, Y. Wang, S. Xue, R. Ge, L. Chen, Y. Liu, A. Huang, X. Fu, P. Xu, T. Yi, F. Xu, M. Deng, J. B. Wang, J. D. A. Meinecke, J. C. F. Matthews, X. Cai, X. Yang, J. Wu, *Sci. Adv.* **2021**, *7*, eabb8375.
- [25] J. Arrazola, V. Bergholm, K. Brádler, T. Bromley, M. Collins, I. Dhand, A. Furnagalli, T. Gerrits, A. Goussev, L. Helt, J. Hundal, T. Isacsson, R. B. Israel, J. Izaac, S. Jahangiri, R. Janik, N. Killoran, S. P. Kumar, J. Lavoie, A. E. Lita, D. H. Mahler, M. Menotti, B. Morrison, S. W. Nam, L. Neuhaus, H. Y. Qi, N. Quesada, A. Repington, K. K. Sabapathy, M. Schuld, *Nature* **2021**, *591*, 54.
- [26] X. Chen, Y. Deng, S. Liu, T. Pramanik, J. Mao, J. Bao, C. Zhai, T. Dai, H. Yuan, J. Guo, S.-M. Fei, M. Huber, B. Tang, Y. Yang, Z. Li, Q. He, Q. Gong, J. Wang, *Nat. Commun.* **2021**, *12*, 2712.
- [27] Y. Qi, Y. Li, *Nanophotonics* **2020**, *9*, 1287.
- [28] H. Jin, F. Liu, P. Xu, J. Xia, M. Zhong, Y. Yuan, J. Zhou, Y. Gong, W. Wang, S. Zhu, *Phys. Rev. Lett.* **2014**, *113*, 103601.
- [29] C. Wang, M. Zhang, X. Chen, M. Bertrand, A. Shams-Ansari, S. Chandrasekhar, P. Winzer, M. Lončar, *Nature* **2018**, *562*, 101.
- [30] M. He, M. Xu, Y. Ren, J. Jian, Z. Ruan, Y. Xu, S. Gao, S. Sun, X. Wen, L. Zhou, L. Liu, C. Guo, H. Chen, S. Yu, L. Liu, X. Cai, *Nat. Photonics* **2019**, *13*, 359.
- [31] T. Meany, M. Gräfe, R. Heilmann, A. Perez-Leija, S. Gross, M. J. Steel, M. J. Withford, A. Szameit, *Laser Photonics Rev.* **2015**, *9*, 363.
- [32] G. Goltsman, O. Okunev, G. Chulkova, A. Lipatov, A. Semenov, K. Smirnov, B. Voronov, A. Dzardanov, C. Williams, R. Sobolewski, *Appl. Phys. Lett.* **2001**, *79*, 705.
- [33] A. Sipahigil, R. E. Evans, D. D. Sukachev, M. J. Burek, J. Borregaard, M. K. Bhaskar, C. T. Nguyen, J. L. Pacheco, H. A. Atikian, C. Meuwly, R. M. Camacho, F. Jelezko, E. Bielejec, H. Park, M. Lončar, M. D. Lukin, *Science* **2016**, *354*, 847.
- [34] M. A. Guidry, K. Y. Yang, D. M. Lukin, A. Markosyan, J. Yang, M. M. Fejer, J. Vučković, *Optica* **2020**, *7*, 1139.
- [35] A. Orieux, A. Eckstein, A. Lemaître, P. Filloux, I. Favero, G. Leo, T. Coudreau, A. Keller, P. Milman, S. Ducci, *Phys. Rev. Lett.* **2013**, *110*, 160502.
- [36] W. Xie, L. Chang, H. Shu, J. C. Norman, J. D. Peters, X. Wang, J. E. Bowers, *Opt. Express* **2020**, *28*, 32894.
- [37] J. Wang, S. Paesani, Y. Ding, R. Santagati, P. Skrzypczyk, A. Salavrakos, J. Tura, R. Augusiak, L. Mančinska, D. Bacco, *Science* **2018**, *360*, 285.
- [38] S. Paesani, Y. Ding, R. Santagati, L. Chakhmakhchyan, C. Vigliar, K. Rottwitt, L. K. Oxenløwe, J. Wang, M. G. Thompson, A. Laing, *Nat. Phys.* **2019**, *15*, 925.
- [39] J. Wang, D. Bonneau, M. Villa, J. W. Silverstone, R. Santagati, S. Miki, T. Yamashita, M. Fujiwara, M. Sasaki, H. Terai, M. G. Tanner, C. M. Natarajan, R. H. Hadfield, J. L. O'Brien, M. G. Thompson, *Optica* **2016**, *3*, 407.
- [40] P. Sibson, J. E. Kennard, S. Stanisic, C. Erven, J. L. O'Brien, M. G. Thompson, *Optica* **2017**, *4*, 172.
- [41] G. Zhang, J. Haw, H. Cai, F. Xu, S. Assad, J. Fitzsimons, X. Zhou, Y. Zhang, S. Yu, J. Wu, W. Ser, L. C. Kwek, A. Q. Liu, *Nat. Photonics* **2019**, *13*, 839.
- [42] K. Wei, W. Li, H. Tan, Y. Li, H. Min, W.-J. Zhang, H. Li, L. You, Z. Wang, X. Jiang, T.-Y. Chen, S.-K. Liao, C.-Z. Peng, F. Xu, J.-W. Pan, *Phys. Rev. X* **2020**, *10*, 031030.
- [43] A. H. Atabaki, S. Moazeni, F. Pavanello, H. Gevorgyan, J. Notaros, L. Alloatti, M. T. Wade, C. Sun, S. A. Kruger, H. Meng, K. A. Qubaisi, I. Wang, B. Zhang, A. Khilo, C. V. Baiocco, M. A. Popović, V. M. Stojanović, R. J. Ram, *Nature* **2018**, *556*, 349.
- [44] J. C. Adcock, J. Bao, Y. Chi, X. Chen, D. Bacco, Q. Gong, L. K. Oxenløwe, J. Wang, Y. Ding, *IEEE J. Sel. Top. Quantum Electron.* **2020**, *27*, 6700224.
- [45] J. W. Silverstone, D. Bonneau, J. L. O'Brien, M. G. Thompson, *IEEE J. Sel. Top. Quantum Electron.* **2016**, *22*, 390.
- [46] S. Bogdanov, M. Shalaginov, A. Boltasseva, V. M. Shalaev, *Opt. Mater. Express* **2017**, *7*, 111.
- [47] M. Giustina, M. A. M. Versteegh, S. Wengerowsky, J. Handsteiner, A. Hochrainer, K. Phelan, F. Steinlechner, J. Kofler, J.-A. Larsson, C. Abellán, W. Amaya, V. Pruneri, M. W. Mitchell, J. Beyer, T. Gerrits, A. E. Lita, L. K. Shalm, S. W. Nam, T. Scheidl, R. Ursin, B. Wittmann, A. Zeilinger, *Phys. Rev. Lett.* **2015**, *115*, 250401.
- [48] L. K. Shalm, E. Meyer-Scott, B. G. Christensen, P. Bierhorst, M. A. Wayne, M. J. Stevens, T. Gerrits, S. Glancy, D. R. Hamel, M. S. Allman, K. J. Coakley, S. D. Dyer, C. Hodge, A. E. Lita, V. B. Verma, C. Lambrocco, E. Tortorici, A. L. Miggall, Y. Zhang, D. R. Kumor, W. H. Farr, F. Marsili, M. D. Shaw, J. A. Stern, C. Abellán, W. Amaya, V. Pruneri, T. Jennewein, M. W. Mitchell, P. G. Kwiat, J. C. Bien-

- fang, R. P. Mirin, E. Knill, S. W. Nam, *Phys. Rev. Lett.* **2015**, *115*, 250402.
- [49] K. Wang, Q. Xu, S. Zhu, X.-s. Ma, *Nat. Photonics* **2019**, *13*, 872.
- [50] X. Ding, Y. He, Z.-C. Duan, N. Gregersen, M.-C. Chen, S. Unsleber, S. Maier, C. Schneider, M. Kamp, S. Höfling, C.-Y. Lu, J.-W. Pan, *Phys. Rev. Lett.* **2016**, *116*, 020401.
- [51] N. Somaschi, V. Giesz, L. De Santis, J. Loredo, M. P. Almeida, G. Hornecker, S. L. Portalupi, T. Grange, C. Antón, J. Demory, C. Gómez, I. Sagues, N. D. Lanzillotti-Kimura, A. Lemaitre, A. Auf- feves, A. G. White, L. Lanço, P. Senellart, *Nat. Photonics* **2016**, *10*, 340.
- [52] Ł. Dusanowski, S.-H. Kwon, C. Schneider, S. Höfling, *Phys. Rev. Lett.* **2019**, *122*, 173602.
- [53] J.-Y. Chen, Z.-H. Ma, Y. M. Sua, Z. Li, C. Tang, Y.-P. Huang, *Optica* **2019**, *6*, 1244.
- [54] J. Zhao, C. Ma, M. Rüsing, S. Mookherjea, *Phys. Rev. Lett.* **2020**, *124*, 163603.
- [55] G.-T. Xue, Y.-F. Niu, X. Liu, J.-C. Duan, W. Chen, Y. Pan, K. Jia, X. Wang, H.-Y. Liu, Y. Zhang, P. Xu, G. Zhao, X. Cai, Y.-X. Gong, X. Hu, Z. Xie, S. Zhu, *Phys. Rev. Appl.* **2021**, *15*, 064059.
- [56] Z. Ma, J.-Y. Chen, Z. Li, C. Tang, Y. M. Sua, H. Fan, Y.-P. Huang, *Phys. Rev. Lett.* **2020**, *125*, 263602.
- [57] X. Guo, C.-I. Zou, C. Schuck, H. Jung, R. Cheng, H. X. Tang, *Light Sci. Appl.* **2017**, *6*, e16249.
- [58] C. Reimer, M. Kues, P. Roztocki, B. Wetzel, F. Grazioso, B. E. Little, S. T. Chu, T. Johnston, Y. Bromberg, L. Caspani, D. J. Moss, R. Morandotti, *Science* **2016**, *351*, 1176.
- [59] X. Lu, Q. Li, D. A. Westly, G. Moille, A. Singh, V. Anant, S. Kartik, *Nat. Phys.* **2019**, *15*, 373.
- [60] W. Bogaerts, P. De Heyn, T. Van Vaerenbergh, K. De Vos, S. Kumar Selvaraja, T. Claes, P. Dumon, P. Bienstman, D. Van Thourhout, R. Baets, *Laser Photonics Rev.* **2012**, *6*, 47.
- [61] Y. Guo, W. Zhang, N. Lv, Q. Zhou, Y. Huang, J. Peng, *Opt. Express* **2014**, *22*, 2620.
- [62] B. M. Burridge, I. I. Faruque, J. G. Rarity, J. Barreto, *Opt. Lett.* **2020**, *45*, 4048.
- [63] P. Imany, J. A. Jaramillo-Villegas, O. D. Odele, K. Han, D. E. Leaird, J. M. Lukens, P. Lougovski, M. Qi, A. M. Weiner, *Opt. Express* **2018**, *26*, 1825.
- [64] Q. Lin, O. J. Painter, G. P. Agrawal, *Opt. Express* **2007**, *15*, 16604.
- [65] J. E. Sharping, K. F. Lee, M. A. Foster, A. C. Turner, B. S. Schmidt, M. Lipson, A. L. Gaeta, P. Kumar, *Opt. Express* **2006**, *14*, 12388.
- [66] X. Qiang, X. Zhou, J. Wang, C. M. Wilkes, T. Loke, S. O'Gara, L. Kling, G. D. Marshall, R. Santagati, T. C. Ralph, J. B. Wang, J. L. O'Brien, Mark G. Thompson, J. C. F. Matthews, *Nat. Photonics* **2018**, *12*, 534.
- [67] J. W. Silverstone, D. Bonneau, K. Ohira, N. Suzuki, H. Yoshida, N. Iizuka, M. Ezaki, C. M. Natarajan, M. G. Tanner, R. H. Hadfield, V. Zwiller, G. D. Marshall, J. G. Rarity, J. L. O'Brien, M. G. Thompson, *Nat. Photon.* **2014**, *8*, 104.
- [68] L.-T. Feng, M. Zhang, Z.-Y. Zhou, Y. Chen, M. Li, D.-X. Dai, H.-L. Ren, G.-P. Guo, G.-C. Guo, M. Tame, X.-F. Ren, *npj Quantum Inf.* **2019**, *5*, 90.
- [69] J. C. Adcock, C. Vigliar, R. Santagati, J. W. Silverstone, M. G. Thompson, *Nat. Commun.* **2019**, *10*, 3528.
- [70] C. Vigliar, S. Paesani, Y. Ding, J. C. Adcock, J. Wang, S. Morley-Short, D. Bacco, L. K. Oxenløwe, M. G. Thompson, J. G. Rarity, A. Laing, *Nat. Phys.* **2021**, *17*, 1137.
- [71] E. Engin, D. Bonneau, C. M. Natarajan, A. S. Clark, M. G. Tanner, R. H. Hadfield, S. N. Dorenbos, V. Zwiller, K. Ohira, N. Suzuki, H. Yoshida, N. Iizuka, M. Ezaki, J. L. O'Brien, M. G. Thompson, *Opt. Express* **2013**, *21*, 27826.
- [72] J. W. Silverstone, R. Santagati, D. Bonneau, M. J. Strain, M. Sorel, J. L. O'Brien, M. G. Thompson, *Nat. Commun.* **2015**, *6*, 7948.
- [73] D. Grassani, S. Azzini, M. Liscidini, M. Galli, M. J. Strain, M. Sorel, J. Sipe, D. Bajoni, *Optica* **2015**, *2*, 88.
- [74] R. Wakabayashi, M. Fujiwara, K.-i. Yoshino, Y. Nambu, M. Sasaki, T. Aoki, *Opt. Express* **2015**, *23*, 1103.
- [75] J. B. Christensen, J. G. Koefoed, K. Rottwitt, C. McKinstry, *Opt. Lett.* **2018**, *43*, 859.
- [76] K. Guo, X. Shi, X. Wang, J. Yang, Y. Ding, H. Ou, Y. Zhao, *Photonics Res.* **2018**, *6*, 587.
- [77] C. Tison, J. Steidle, M. Fanto, Z. Wang, N. Mogent, A. Rizzo, S. Preble, P. Alsing, *Opt. Express* **2017**, *25*, 33088.
- [78] Y. Liu, C. Wu, X. Gu, Y. Kong, X. Yu, R. Ge, X. Cai, X. Qiang, J. Wu, X. Yang, P. Xu, *Opt. Lett.* **2020**, *45*, 73.
- [79] L. Lu, L. Xia, Z. Chen, L. Chen, T. Yu, T. Tao, W. Ma, Y. Pan, X. Cai, Y. Lu, S. Zhu, X.-S. Ma, *npj Quantum Inf.* **2020**, *6*, 30.
- [80] M. J. Strain, C. Lacava, L. Meriggi, I. Cristiani, M. Sorel, *Opt. Lett.* **2015**, *40*, 1274.
- [81] L. Zhang, L. Jie, M. Zhang, Y. Wang, Y. Xie, Y. Shi, D. Dai, *Photonics Res.* **2020**, *8*, 684.
- [82] C. A. Husko, A. S. Clark, M. J. Collins, A. De Rossi, S. Combrié, G. Lehocq, I. H. Rey, T. F. Krauss, C. Xiong, B. J. Eggleton, *Sci. Rep.* **2013**, *3*, 3087.
- [83] F. Da Ros, D. Vukovic, A. Gajda, K. Dalgaard, L. Zimmermann, B. Tillack, M. Galili, K. Petermann, C. Peucheret, *Opt. Express* **2014**, *22*, 5029.
- [84] C. Ma, S. Mookherjea, *OSA Continuum* **2020**, *3*, 1138.
- [85] L. M. Rosenfeld, D. A. Sulway, G. F. Sinclair, V. Anant, M. G. Thompson, J. G. Rarity, J. W. Silverstone, *Opt. Express* **2020**, *28*, 37092.
- [86] S. Ramelow, A. Farsi, S. Clemmen, D. Orquiza, K. Luke, M. Lipson, A. L. Gaeta, arXiv:1508.04358, **2015**.
- [87] F. Samara, A. Martin, C. Autebert, M. Karpov, T. J. Kippenberg, H. Zbinden, R. Thew, *Opt. Express* **2019**, *27*, 19309.
- [88] F. Samara, N. Maring, A. Martin, A. Raja, T. Kippenberg, H. Zbinden, R. Thew, *Quantum Sci. Technol.* **2021**, *6*, 045024.
- [89] M. Kues, C. Reimer, P. Roztocki, L. R. Cortes, S. Sciara, B. Wetzel, Y. Zhang, A. Cino, S. T. Chu, B. E. Little, D. J. Moss, L. Caspani, J. Azaña, R. Morandotti, *Nature* **2017**, *546*, 622.
- [90] C. Reimer, S. Sciara, P. Roztocki, M. Islam, L. R. Cortés, Y. Zhang, B. Fischer, S. Loranger, R. Kashyap, A. Cino, *Nat. Phys.* **2019**, *15*, 148.
- [91] P. Senellart, G. Solomon, A. White, *Nat. Nanotechnol.* **2017**, *12*, 1026.
- [92] X. He, N. F. Hartmann, X. Ma, Y. Kim, R. Ihly, J. L. Blackburn, W. Gao, J. Kono, Y. Yomogida, A. Hirano, T. Tanaka, H. Kataura, H. Htoon, S. K. Doorn, *Nat. Photonics* **2017**, *11*, 577.
- [93] T. T. Tran, D. Wang, Z.-Q. Xu, A. Yang, M. Toth, T. W. Odom, I. Aharonovich, *Nano Lett.* **2017**, *17*, 2634.
- [94] F. DellAnno, S. De Siena, F. Illuminati, *Phys. Rep.* **2006**, *428*, 53.
- [95] J. E. Froch, S. Kim, C. Stewart, X. Xu, Z. Du, M. Lockrey, M. Toth, I. Aharonovich, *Nano Lett.* **2020**, *20*, 2784.
- [96] Y. Chen, A. Ryoo, M. R. Friedfeld, T. Fryett, J. Whitehead, B. M. Cosairt, A. Majumdar, *Nano Lett.* **2018**, *18*, 6404.
- [97] J. Q. Grim, A. S. Bracker, M. Zalalutdinov, S. G. Carter, A. C. Kozen, M. Kim, C. S. Kim, J. T. Mlack, M. Yakes, B. Lee, D. Gammon, *Nat. Mater.* **2019**, *18*, 963.
- [98] A. Eich, T. C. Spiekermann, H. Gehring, L. Sommer, J. R. Bankwitz, P. P. Schrinner, J. A. Preuß, S. M. de Vasconcellos, R. Bratschitsch, W. H. Pernice, C. Schuck, arXiv:2104.11830, **2021**.
- [99] A. Senichev, Z. O. Martin, S. Peana, D. Sychev, X. Xu, A. S. Lagutchev, A. Boltasseva, V. M. Shalaev, arXiv:2104.08128, **2021**.
- [100] L. Caspani, C. Xiong, B. J. Eggleton, D. Bajoni, M. Liscidini, M. Galli, R. Morandotti, D. J. Moss, *Light Sci. Appl.* **2017**, *6*, e17100.
- [101] S. Signorini, L. Pavese, AVS Quantum Sci. **2020**, *2*, 041701.
- [102] A. Christ, C. Silberhorn, *Phys. Rev. A* **2012**, *85*, 023829.
- [103] J. Tiedau, T. J. Bartley, G. Harder, A. E. Lita, S. W. Nam, T. Gerrits, C. Silberhorn, *Phys. Rev. A* **2019**, *100*, 041802.

- [104] E. Meyer-Scott, C. Silberhorn, A. Migdall, *Rev. Sci. Instrum.* **2020**, *91*, 041101.
- [105] A. M. Brańczyk, A. Fedrizzi, T. M. Stace, T. C. Ralph, A. G. White, *Opt. Express* **2011**, *19*, 55.
- [106] F. Kaneda, K. Garay-Palmett, A. B. URen, P. G. Kwiat, *Opt. Express* **2016**, *24*, 10733.
- [107] F. Graffitti, D. Kundys, D. T. Reid, A. M. Brańczyk, A. Fedrizzi, *Quantum Sci. Technol.* **2017**, *2*, 035001.
- [108] F. Graffitti, P. Barrow, M. Proietti, D. Kundys, A. Fedrizzi, *Optica* **2018**, *5*, 514.
- [109] V. Ansari, J. M. Donohue, B. Brecht, C. Silberhorn, *Optica* **2018**, *5*, 534.
- [110] S. Slussarenko, G. J. Pryde, *Appl. Phys. Rev.* **2019**, *6*, 041303.
- [111] Y.-C. Liu, D.-J. Guo, K.-Q. Ren, R. Yang, M. Shang, W. Zhou, X. Li, C.-W. Sun, P. Xu, Z. Xie, Y.-X. Gong, S.-N. Zhu, *Sci. Rep.* **2021**, *11*, 12628.
- [112] M. A. Foster, A. C. Turner, J. E. Sharping, B. S. Schmidt, M. Lipson, A. L. Gaeta, *Nature* **2006**, *441*, 960.
- [113] N. Matsuda, H. Le Jeannic, H. Fukuda, T. Tsuchizawa, W. J. Munro, K. Shimizu, K. Yamada, Y. Tokura, H. Takesue, *Sci. Rep.* **2012**, *2*, 817.
- [114] S. Signorini, M. Mancinelli, M. Borghi, M. Bernard, M. Ghulinyan, G. Pucker, L. Pavesi, *Photonics Res.* **2018**, *6*, 805.
- [115] L.-T. Feng, M. Zhang, X. Xiong, Y. Chen, H. Wu, M. Li, G.-P. Guo, G.-C. Guo, D.-X. Dai, X.-F. Ren, *npj Quantum Inf.* **2019**, *5*, 1.
- [116] S. Paesani, M. Borghi, S. Signorini, A. Maños, L. Pavesi, A. Laing, *Nat. Commun.* **2020**, *11*, 2505.
- [117] J. B. Spring, P. L. Mennea, B. J. Metcalf, P. C. Humphreys, J. C. Gates, H. L. Rogers, C. Söller, B. J. Smith, W. S. Kolthammer, P. G. Smith, I. A. Walmsley, *Optica* **2017**, *4*, 90.
- [118] Z. Vernon, M. Liscidini, J. E. Sipe, *Opt. Lett.* **2016**, *41*, 788.
- [119] A. I. Lvovsky, *Photonics: Scientific Foundations, Technology and Applications* (Ed: D. L. Andrews), Wiley, New York **2015**, pp. 121–163.
- [120] U. L. Andersen, T. Gehring, C. Marquardt, G. Leuchs, *Phys. Scr.* **2016**, *91*, 053001.
- [121] M. e. Tse, H. Yu, N. Kijbunchoo, A. Fernandez-Galiana, P. Dupej, L. Barsotti, C. Blair, D. Brown, S. Dwyer, A. Effler, M. Evans, P. Fritschel, V. V. Frolov, A. C. Green, G. L. Mansell, F. Matichard, N. Mavalvala, D. E. McClelland, L. McCuller, T. McRae, J. Miller, A. Mullavey, E. Oelker, I. Y. Phinney, D. Sigg, B. J. J. Slagmolen, T. Vo, R. L. Ward, C. Whittle, R. Abbott, et al., *Phys. Rev. Lett.* **2019**, *123*, 231107.
- [122] V. Giovannetti, S. Lloyd, L. Maccone, *Science* **2004**, *306*, 1330.
- [123] C. Weedbrook, S. Pirandola, R. García-Patrón, N. J. Cerf, T. C. Ralph, J. H. Shapiro, S. Lloyd, *Rev. Mod. Phys.* **2012**, *84*, 621.
- [124] S. Takeda, A. Furusawa, *APL Photonics* **2019**, *4*, 060902.
- [125] L.-A. Wu, H. Kimble, J. Hall, H. Wu, *Phys. Rev. Lett.* **1986**, *57*, 2520.
- [126] R. M. Shelby, M. D. Levenson, S. H. Perlmutter, R. G. DeVoe, D. F. Walls, *Phys. Rev. Lett.* **1986**, *57*, 691.
- [127] R. Slusher, L. Hollberg, B. Yurke, J. Mertz, J. Valley, *Phys. Rev. Lett.* **1985**, *55*, 2409.
- [128] A. Dutt, K. Luke, S. Manipatruni, A. L. Gaeta, P. Nussenzveig, M. Lipson, *Phys. Rev. Appl.* **2015**, *3*, 044005.
- [129] A. Dutt, S. Miller, K. Luke, J. Cardenas, A. L. Gaeta, P. Nussenzveig, M. Lipson, *Opt. Lett.* **2016**, *41*, 223.
- [130] Z. Vernon, N. Quesada, M. Liscidini, B. Morrison, M. Menotti, K. Tan, J. Sipe, *Phys. Rev. Lett.* **2019**, *12*, 064024.
- [131] A. Otterpohl, F. Sedlmeir, U. Vogl, T. Dirmeier, G. Shafiee, G. Schunk, D. V. Strekalov, H. G. Schwefel, T. Gehring, U. L. Andersen, G. Leuchs, C. Marquardt, *Optica* **2019**, *6*, 1375.
- [132] F. Mondain, T. Lunghi, A. Zavatta, E. Gouzien, F. Doutre, M. De Michelis, S. Tanzilli, V. D'Auria, *Photonics Rev.* **2019**, *7*, A36.
- [133] V. D. Vaidya, B. Morrison, L. Helt, R. Shahrokshahi, D. Mahler, M. Collins, K. Tan, J. Lavoie, A. Repington, M. Menotti, N. Quesada, R. C. Pooser, A. E. Lita, T. Gerrits, S. W. Nam, Z. Vernon, *Sci. Adv.* **2020**, *6*, eaba9186.
- [134] Y. Zhao, Y. Okawachi, J. K. Jang, X. Ji, M. Lipson, A. L. Gaeta, *Phys. Rev. Lett.* **2020**, *124*, 193601.
- [135] Y. Zhang, M. Menotti, K. Tan, V. Vaidya, D. Mahler, L. Helt, L. Zatti, M. Liscidini, B. Morrison, Z. Vernon, *Nat. Commun.* **2021**, *12*, 2233.
- [136] S. Chung, H. Abediasl, H. Hashemi, *IEEE J. Solid State Circuits* **2017**, *53*, 275.
- [137] J. Carolan, C. Harrold, C. Sparrow, E. Martín-López, N. J. Russell, J. W. Silverstone, P. J. Shadbolt, N. Matsuda, M. Oguma, M. Itoh, G. D. Marshall, M. G. Thompson, J. C. F. Matthews, T. Hashimoto, J. L. O'Brien, A. Laing, *Science* **2015**, *349*, 711.
- [138] Y. Shen, N. C. Harris, S. Skirlo, M. Prabhu, T. Baehr-Jones, M. Hochberg, X. Sun, S. Zhao, H. Larochelle, D. Englund, M. Soljačić, *Nat. Photonics* **2017**, *11*, 441.
- [139] J. Notaros, J. Mower, M. Heuck, C. Lupo, N. C. Harris, G. R. Steinbrecher, D. Bunandar, T. Baehr-Jones, M. Hochberg, S. Lloyd, D. Englund, *Opt. Express* **2017**, *25*, 21275.
- [140] M. Reck, A. Zeilinger, H. J. Bernstein, P. Bertani, *Phys. Rev. Lett.* **1994**, *73*, 58.
- [141] W. R. Clements, P. C. Humphreys, B. J. Metcalf, W. S. Kolthammer, I. A. Walmsley, *Optica* **2016**, *3*, 1460.
- [142] P. Dumais, Y. Wei, M. Li, F. Zhao, X. Tu, J. Jiang, D. Celo, D. J. Goodwill, H. Fu, D. Geng, E. Bernier, *Optical Fiber Communication Conference*, Optical Society of America, Washington, D.C **2016**, p. W2A.19.
- [143] A. Biberman, M. J. Shaw, E. Timurdogan, J. B. Wright, M. R. Watts, *Opt. Lett.* **2012**, *37*, 4236.
- [144] C. M. Wilkes, X. Qiang, J. Wang, R. Santagati, S. Paesani, X. Zhou, D. A. Miller, G. D. Marshall, M. G. Thompson, J. L. O'Brien, *Opt. Lett.* **2016**, *41*, 5318.
- [145] T. Rudolph, *APL Photonics* **2017**, *2*, 030901.
- [146] N. C. Harris, Y. Ma, J. Mower, T. Baehr-Jones, D. Englund, M. Hochberg, C. Galland, *Opt. Express* **2014**, *22*, 10487.
- [147] M. Gehl, C. Long, D. Trotter, A. Starbuck, A. Pomerene, J. B. Wright, S. Melgaard, J. Siiriola, A. L. Lentine, C. DeRose, *Optica* **2017**, *4*, 374.
- [148] S. Abel, F. Eltes, J. E. Ortmann, A. Messner, P. Castera, T. Wagner, D. Urbonas, A. Rosa, A. M. Gutierrez, D. Tulli, P. Ma, B. Baeuerle, A. Josten, W. Heni, D. Caimi, L. Czornomaz, A. A. Demkov, J. Leuthold, P. Sanchis, J. Fompeyrine, *Nat. Mater.* **2019**, *18*, 42.
- [149] U. Chakraborty, J. Carolan, G. Clark, D. Bunandar, G. Gilbert, J. Notaros, M. R. Watts, D. R. Englund, *Optica* **2020**, *7*, 1385.
- [150] A. Atabaki, E. S. Hosseini, A. Eftekhar, S. Yegnanarayanan, A. Adibi, *Opt. Express* **2010**, *18*, 18312.
- [151] S. Gao, H. Lin, L. Zhou, L. Liu, M. He, J. Xu, L. Chen, Y. Luo, X. Cai, *IEEE Photon. Technol. Lett.* **2019**, *31*, 537.
- [152] T. Baehr-Jones, R. Ding, Y. Liu, A. Ayazi, T. Pinguet, N. C. Harris, M. Streshinsky, P. Lee, Y. Zhang, A. E.-J. Lim, T.-Y. Liow, S. H.-G. Teo, G.-Q. Lo, M. Hochberg, *Opt. Express* **2012**, *20*, 12014.
- [153] S. Abel, D. Caimi, M. Sousa, T. Stöferle, C. Rossel, C. Marchiori, A. Chelnokov, J. Fompeyrine, *Oxide-based Materials and Devices III* (Eds: F. H. Teherani, D. C. Look, D. J. Rogers), Proc. SPIE Vol. 8263, SPIE, Washington, D.C **2012**, p. 82630Y.
- [154] C. M. Natarajan, M. G. Tanner, R. H. Hadfield, *Supercond. Sci. Technol.* **2012**, *25*, 063001.
- [155] S. Ferrari, C. Schuck, W. Pernice, *Nanophotonics* **2018**, *7*, 1725.
- [156] W. H. Pernice, C. Schuck, O. Minaeva, M. Li, G. Goltsman, A. Sergienko, H. Tang, *Nat. Commun.* **2012**, *3*, 1325.
- [157] F. Najafi, J. Mower, N. C. Harris, F. Bellei, A. Dane, C. Lee, X. Hu, P. Kharel, F. Marsili, S. Assefa, K. K Berggren, D. Englund, *Nat. Commun.* **2015**, *6*, 5873.
- [158] M. K. Akhlaghi, E. Schelew, J. F. Young, *Nat. Commun.* **2015**, *6*, 8233.
- [159] S. Gyger, J. Zichi, L. Schweikert, A. W. Elshaari, S. Steinhauer, S. F. Covre da Silva, A. Rastelli, V. Zwiller, K. D. Jöns, C. Errando-Herranz, *Nat. Commun.* **2021**, *12*, 1408.

- [160] S. Buckley, J. Chiles, A. N. McCaughan, G. Moody, K. L. Silverman, M. J. Stevens, R. P. Mirin, S. W. Nam, J. M. Shainline, *Appl. Phys. Lett.* **2017**, *111*, 141101.
- [161] J. Li, R. A. Kirkwood, L. J. Baker, D. Bosworth, K. Erotokritou, A. Banerjee, R. M. Heath, C. M. Natarajan, Z. H. Barber, M. Sorel, R. H. Hadfield, *Opt. Express* **2016**, *24*, 13931.
- [162] E. Lomonte, M. A. Wolff, F. Beutel, S. Ferrari, C. Schuck, W. H. Pernice, F. Lenzini, arXiv:2103.10973, **2021**.
- [163] D. V. Reddy, R. R. Nerem, S. W. Nam, R. P. Mirin, V. B. Verma, *Optica* **2020**, *7*, 1649.
- [164] J. Münzberg, A. Vetter, F. Beutel, W. Hartmann, S. Ferrari, W. H. Pernice, C. Rockstuhl, *Optica* **2018**, *5*, 658.
- [165] B. Korzh, Q.-Y. Zhao, J. P. Allmaras, S. Frasca, T. M. Autry, E. A. Bersin, A. D. Beyer, R. M. Briggs, B. Bumble, M. Colangelo, G. M. Crouch, A. E. Dane, T. Gerrits, A. E. Lita, F. Marsili, G. Moody, C. Peña, E. Ramirez, J. D. Rezac, N. Sinclair, M. J. Stevens, A. E. Velasco, V. B. Verma, E. E. Wollman, S. Xie, D. Zhu, P. D. Hale, M. Spiropulu, K. L. Silverman, R. P. Mirin, et al., *Nat. Photonics* **2020**, *14*, 250.
- [166] C. Schuck, W. H. Pernice, H. X. Tang, *Sci. Rep.* **2013**, *3*, 1893.
- [167] E. E. Wollman, V. B. Verma, A. E. Lita, W. H. Farr, M. D. Shaw, R. P. Mirin, S. W. Nam, *Opt. Express* **2019**, *27*, 35279.
- [168] Q.-Y. Zhao, D. Zhu, N. Calandri, A. E. Dane, A. N. McCaughan, F. Bellei, H.-Z. Wang, D. F. Santavicca, K. K. Berggren, *Nat. Photonics* **2017**, *11*, 247.
- [169] X. Tao, H. Hao, X. Li, S. Chen, L. Wang, X. Tu, X. Jia, L. Zhang, Q. Zhao, L. Kang, P. Wu, *IEEE Photonics J.* **2020**, *12*, 4501308.
- [170] D. Zhu, Q.-Y. Zhao, H. Choi, T.-J. Lu, A. E. Dane, D. Englund, K. K. Berggren, *Nat. Nanotechnol.* **2018**, *13*, 596.
- [171] D. Zhu, M. Colangelo, C. Chen, B. A. Korzh, F. N. Wong, M. D. Shaw, K. K. Berggren, *Nano Lett.* **2020**, *20*, 3858.
- [172] R. Cheng, C.-L. Zou, X. Guo, S. Wang, X. Han, H. X. Tang, *Nat. Commun.* **2019**, *10*, 4104.
- [173] F. Beutel, H. Gehring, M. A. Wolff, C. Schuck, W. Pernice, *npj Quantum Inf.* **2021**, *7*, 40.
- [174] P. Zhang, X. Zheng, R. Ge, L. Lu, Q. Chen, F. Qu, L. Zhang, X. Cai, Y. Lu, S. Zhu, P. Wu, X.-S. Ma, arXiv:1912.09642, **2019**.
- [175] A. C. Dada, J. Leach, G. S. Buller, M. J. Padgett, E. Andersson, *Nat. Phys.* **2011**, *7*, 677.
- [176] X.-L. Wang, X.-D. Cai, Z.-E. Su, M.-C. Chen, D. Wu, L. Li, N.-L. Liu, C.-Y. Lu, J.-W. Pan, *Nature* **2015**, *518*, 516.
- [177] C. Schaeff, R. Polster, M. Huber, S. Ramelow, A. Zeilinger, *Optica* **2015**, *2*, 523.
- [178] R. Thew, A. Acín, H. Zbinden, N. Gisin, *Quantum Inf. Comput.* **2004**, *4*, 93.
- [179] D. Richart, Y. Fischer, H. Weinfurter, *Appl. Phys. B* **2012**, *106*, 543.
- [180] A. Polit, M. J. Cryan, J. G. Rarity, S. Yu, J. L. O'Brien, *Science* **2008**, *320*, 646.
- [181] J. Zeuner, A. N. Sharma, M. Tillmann, R. Heilmann, M. Gräfe, A. Moqanaki, A. Szameit, P. Walther, *npj Quantum Inf.* **2018**, *4*, 13.
- [182] A. Polit, J. C. Matthews, M. G. Thompson, J. L. O'Brien, *IEEE J. Sel. Top. Quantum Electron.* **2009**, *15*, 1673.
- [183] M. Reck, A. Zeilinger, H. J. Bernstein, P. Bertani, *Phys. Rev. Lett.* **1994**, *73*, 58.
- [184] J. Mower, N. C. Harris, G. R. Steinbrecher, Y. Lahini, D. Englund, *Phys. Rev. A* **2015**, *92*, 032322.
- [185] D. A. Miller, *Optica* **2015**, *2*, 747.
- [186] S. Flidzhyan, M. Y. Saygin, S. Kulik, *Opt. Lett.* **2020**, *45*, 2632.
- [187] N. C. Harris, G. R. Steinbrecher, M. Prabhu, Y. Lahini, J. Mower, D. Burandar, C. Chen, F. N. Wong, T. Baehr-Jones, M. Hochberg, S. Lloyd, D. Englund, *Nat. Photonics* **2017**, *11*, 447.
- [188] D. Pérez, I. Gasulla, L. Crudgington, D. J. Thomson, A. Z. Khokhar, K. Li, W. Cao, G. Z. Mashanovich, J. Capmany, *Nat. Commun.* **2017**, *8*, 636.
- [189] M. Prabhu, C. Roques-Carmes, Y. Shen, N. Harris, L. Jing, J. Carolan, R. Hamerly, T. Baehr-Jones, M. Hochberg, V. Čepičić, J. D. Joannopoulos, D. R. Englund, M. Soljačić, *Optica* **2020**, *7*, 551.
- [190] J. Carolan, M. Mohseni, J. P. Olson, M. Prabhu, C. Chen, D. Burandar, M. Y. Niu, N. C. Harris, F. N. Wong, M. Hochberg, S. Lloyd, D. Englund, *Nat. Phys.* **2020**, *16*, 322.
- [191] C. Sparrow, E. Martín-López, N. Maraviglia, A. Neville, C. Harrold, J. Carolan, Y. N. Joglekar, T. Hashimoto, N. Matsuda, J. L. O'Brien, D. P. Tew, A. Laing, *Nature* **2018**, *557*, 660.
- [192] V. D'Ambrosio, E. Nagali, S. P. Walborn, L. Aolita, S. Slussarenko, L. Marrucci, F. Sciarrino, *Nat. Commun.* **2012**, *3*, 961.
- [193] T. M. Graham, H. J. Bernstein, T.-C. Wei, M. Junge, P. G. Kwiat, *Nat. Commun.* **2015**, *6*, 7185.
- [194] Y.-H. Luo, H.-S. Zhong, M. Erhard, X.-L. Wang, L.-C. Peng, M. Krenn, X. Jiang, L. Li, N.-L. Liu, C.-Y. Lu, A. Zeilinger, J.-W. Pan, *Phys. Rev. Lett.* **2019**, *123*, 070505.
- [195] X.-M. Hu, C. Zhang, B.-H. Liu, Y. Cai, X.-J. Ye, Y. Guo, W.-B. Xing, C.-X. Huang, Y.-F. Huang, C.-F. Li, G.-C. Guo, *Phys. Rev. Lett.* **2020**, *125*, 230501.
- [196] B. P. Lanyon, M. Barbieri, M. P. Almeida, T. Jennewein, T. C. Ralph, K. J. Resch, G. J. Pryde, J. L. O'Brien, A. Gilchrist, A. G. White, *Nat. Phys.* **2008**, *5*, 134.
- [197] S. Paesani, J. F. Bulmer, A. E. Jones, R. Santagati, A. Laing, *Phys. Rev. Lett.* **2021**, *126*, 230504.
- [198] M. Neeley, M. Ansmann, R. C. Bialczak, M. Hofheinz, E. Lucero, A. D. O'Connell, D. Sank, H. Wang, J. Wenner, A. N. Cleland, *Science* **2009**, *325*, 722.
- [199] T. Vértesi, S. Pironio, N. Brunner, *Phys. Rev. Lett.* **2010**, *104*, 060401.
- [200] R. Lapkiewicz, P. Li, C. Schaeff, N. K. Langford, S. Ramelow, M. Wiesniak, A. Zeilinger, *Nature* **2011**, *474*, 490.
- [201] C. Schaeff, R. Polster, R. Lapkiewicz, R. Fickler, S. Ramelow, A. Zeilinger, *Opt. Express* **2012**, *20*, 16145.
- [202] J. W. Silverstone, D. Bonneau, J. L. O'Brien, M. G. Thompson, *IEEE J. Sel. Top. Quantum Electron.* **2016**, *22*, 390.
- [203] J. W. Silverstone, R. Santagati, D. Bonneau, M. J. Strain, M. Sorel, J. L. O'Brien, M. G. Thompson, *Nat. Commun.* **2015**, *6*, 7948.
- [204] R. Santagati, J. Wang, A. A. Gentile, S. Paesani, N. Wiebe, J. R. McClean, S. Morley-Short, P. J. Shadbolt, D. Bonneau, J. W. Silverstone, D. P. Tew, X. Zhou, J. L. O'Brien, M. G. Thompson, *Sci. Adv.* **2018**, *4*, eaap9646.
- [205] J. Wang, S. Paesani, R. Santagati, S. Knauer, A. A. Gentile, N. Wiebe, M. Petruzzella, J. L. O'Brien, J. G. Rarity, A. Laing, M. G. Thompson, *Nat. Phys.* **2017**, *13*, 551.
- [206] S. Paesani, A. A. Gentile, R. Santagati, J. Wang, N. Wiebe, D. P. Tew, J. L. O'Brien, M. G. Thompson, *Phys. Rev. Lett.* **2017**, *118*, 100503.
- [207] L. G. Valiant, *Theor. Comput. Sci.* **1979**, *8*, 189.
- [208] M. Krenn, X. Gu, A. Zeilinger, *Phys. Rev. Lett.* **2017**, *119*, 240403.
- [209] N. Khaneja, S. J. Glaser, *Chem. Phys.* **2001**, *267*, 11.
- [210] Z. Xie, T. Zhong, S. Shrestha, X. Xu, J. Liang, Y.-X. Gong, J. C. Bienfang, A. Restelli, J. H. Shapiro, F. N. Wong, C. W. Wong, *Nat. Photonics* **2015**, *9*, 536.
- [211] I. I. Faruque, G. F. Sinclair, D. Bonneau, J. G. Rarity, M. G. Thompson, *Opt. Express* **2018**, *26*, 20379.
- [212] D. Llewellyn, Y. Ding, I. I. Faruque, S. Paesani, D. Bacco, R. Santagati, Y.-J. Qian, Y. Li, Y.-F. Xiao, M. Huber, M. Malik, G. F. Sinclair, X. Zhou, K. Rottwitt, J. L. O'Brien, J. G. Rarity, Q. Gong, L. K. Oxenlowe, J. Wang, M. G. Thompson, *Nat. Phys.* **2020**, *16*, 148.
- [213] D. E. Browne, T. Rudolph, *Phys. Rev. Lett.* **2005**, *95*, 010501.
- [214] D. Bouwmeester, J.-W. Pan, K. Mattle, M. Eibl, H. Weinfurter, A. Zeilinger, *Nature* **1997**, *390*, 575.
- [215] M. Malik, M. Erhard, M. Huber, M. Krenn, R. Fickler, A. Zeilinger, *Nat. Photonics* **2016**, *10*, 248.
- [216] L.-T. Feng, M. Zhang, D. Liu, Y.-J. Cheng, G.-P. Guo, D.-X. Dai, G.-C. Guo, M. Krenn, X.-F. Ren, arXiv:2103.14277, **2021**.

- [217] J. B. Spring, B. J. Metcalf, P. C. Humphreys, W. S. Kolthammer, X.-M. Jin, M. Barbieri, A. Datta, N. Thomas-Peter, N. K. Langford, D. Kundys, J. C. Gates, B. J. Smith, P. G. R. Smith, I. A. Walmsley, *Science* **2013**, *339*, 798.
- [218] M. A. Broome, A. Fedrizzi, S. Rahimi-Keshari, J. Dove, S. Aaronson, T. C. Ralph, A. G. White, *Science* **2013**, *339*, 794.
- [219] M. Tillmann, B. Dakić, R. Heilmann, S. Nolte, A. Szameit, P. Walther, *Nat. Photonics* **2013**, *7*, 540.
- [220] H. Wang, Y. He, Y.-H. Li, Z.-E. Su, B. Li, H.-L. Huang, X. Ding, M.-C. Chen, C. Liu, J. Qin, J.-P. Li, Y.-M. He, C. Schneider, M. Kamp, C.-Z. Peng, S. Höfling, C.-Y. Lu, J.-W. Pan, *Nat. Photonics* **2017**, *11*, 361.
- [221] S. Aaronson, A. Arkhipov, *Proceedings of the Forty-Third Annual ACM Symposium on Theory of Computing*, ACM Press, New York **2011**, pp. 333–342.
- [222] J. Huh, G. G. Guerreschi, B. Peropadre, J. R. McClean, A. Aspuru-Guzik, *Nat. Photon.* **2015**, *9*, 615.
- [223] H.-K. Lo, H. F. Chau, *Science* **1999**, *283*, 2050.
- [224] V. Scarani, H. Bechmann-Pasquinucci, N. J. Cerf, M. Dušek, N. Lütkenhaus, M. Peev, *Rev. Mod. Phys.* **2009**, *81*, 1301.
- [225] F. Xu, X. Ma, Q. Zhang, H.-K. Lo, J.-W. Pan, *Rev. Mod. Phys.* **2020**, *92*, 025002.
- [226] S. Pirandola, U. L. Andersen, L. Banchi, M. Berta, D. Bunandar, R. Colbeck, D. Englund, T. Gehring, C. Lupo, C. Ottaviani, J. L. Pereira, M. Razavi, J. S. Shaari, M. Tomamichel, V. C. Usenko, G. Vallone, P. Villoresi, P. Wallden, *Adv. Opt. Photonics* **2020**, *12*, 1012.
- [227] J. F. Tasker, J. Frazer, G. Ferranti, E. J. Allen, L. F. Brunel, S. Tanzilli, V. D'Auria, J. C. Matthews, *Nat. Photonics* **2021**, *15*, 11.
- [228] A. Orieux, E. Diamanti, *J. Opt.* **2016**, *18*, 083002.
- [229] C. Ma, W. D. Sacher, Z. Tang, J. C. Mikkelsen, Y. Yang, F. Xu, T. Thiessen, H.-K. Lo, J. K. Poon, *Optica* **2016**, *3*, 1274.
- [230] F. Mazeas, M. Traetta, M. Bentivegna, F. Kaiser, D. Aktas, W. Zhang, C. A. Ramos, L. Ngah, T. Lunghi, E. Picholle, N. Belabas-Plougonven, X. Le Roux, É. Cassan, D. Marris-Morini, L. Vivien, G. Sauder, L. Labonté, S. Tanzilli, *Opt. Express* **2016**, *24*, 28731.
- [231] C. Autebert, J. Trapateau, A. Orieux, A. Lemaitre, C. Gomez-Carbonell, E. Diamanti, I. Zaquine, S. Ducci, *Quantum Sci. Technol.* **2016**, *1*, 01LT02.
- [232] D. Bacco, Y. Ding, K. Dalgaard, K. Rottwitt, L. K. Oxenløwe, *Sci. Rep.* **2017**, *7*, 12459.
- [233] H. Cai, C. M. Long, C. T. DeRose, N. Boynton, J. Urayama, R. Camacho, A. Pomerene, A. L. Starbuck, D. C. Trotter, P. S. Davids, A. L. Lentine, *Opt. Express* **2017**, *25*, 12282.
- [234] Y. Ding, D. Bacco, K. Dalgaard, X. Cai, X. Zhou, K. Rottwitt, L. K. Oxenløwe, *npj Quantum Inf.* **2017**, *3*, 25.
- [235] D. Bunandar, A. Lentine, C. Lee, H. Cai, C. M. Long, N. Boynton, N. Martinez, C. DeRose, C. Chen, M. Grein, D. Trotter, A. Starbuck, A. Pomerene, S. Hamilton, F. N. C. Wong, R. Camacho, P. Davids, J. Urayama, D. Englund, *Phys. Rev. X* **2018**, *8*, 021009.
- [236] C.-Y. Wang, J. Gao, Z.-Q. Jiao, L.-F. Qiao, R.-J. Ren, Z. Feng, Y. Chen, Z.-Q. Yan, Y. Wang, H. Tang, X.-M. Jin, *Opt. Express* **2019**, *27*, 5982.
- [237] H. Semenenko, P. Sibson, A. Hart, M. G. Thompson, J. G. Rarity, C. Erven, *Optica* **2020**, *7*, 238.
- [238] T. K. Paraíso, I. De Marco, T. Roger, D. G. Marangon, J. F. Dynes, M. Lucamarini, Z. Yuan, A. J. Shields, *npj Quantum Inf.* **2019**, *5*, 42.
- [239] M. Avesani, L. Calderaro, M. Schiavon, A. Stanco, C. Agnesi, A. Santamato, M. Zahidy, A. Scriminich, G. Foletto, G. Contestabile, M. Chiesa, D. Rotta, M. Artiglia, A. Montanaro, M. Romagnoli, V. Sorianello, F. Vedovato, G. Vallone, P. Villoresi, arXiv:1907.10039, **2019**.
- [240] F.-X. Wang, W. Wang, R. Niu, X. Wang, C.-L. Zou, C.-H. Dong, B. E. Little, S. T. Chu, H. Liu, P. Hao, S. Liu, S. Wang, Z.-Q. Yin, D.-Y. He, W. Zhang, W. Zhao, Z.-F. Han, G.-C. Guo, W. Chen, *Laser Photonic Rev.* **2020**, *14*, 1900190.
- [241] L. Cao, W. Luo, Y. Wang, J. Zou, R. Yan, H. Cai, Y. Zhang, X. Hu, C. Jiang, W. Fan, X. Q. Zhou, B. Dong, X. S. Luo, G. Q. Lo, Y. X. Wang, Z. W. Xu, S. H. Sun, X. B. Wang, Y. L. Hao, Y. F. Jin, D. L. Kwong, L. C. Kwek, A. Q. Liu, *Phys. Rev. Appl.* **2020**, *14*, 011001.
- [242] V. Makarov, A. Anisimov, J. Skaar, *Phys. Rev. A* **2006**, *74*, 022313.
- [243] Y. Zhao, C.-H. F. Fung, B. Qi, C. Chen, H.-K. Lo, *Phys. Rev. A* **2008**, *78*, 042333.
- [244] L. Lydersen, C. Wiechers, C. Wittmann, D. Elser, J. Skaar, V. Makarov, *Nat. Photonics* **2010**, *4*, 686.
- [245] M. Elezov, R. Ozhegov, G. Goltsman, V. Makarov, *Opt. Express* **2019**, *27*, 30979.
- [246] S. L. Braunstein, S. Pirandola, *Phys. Rev. Lett.* **2012**, *108*, 130502.
- [247] H.-K. Lo, M. Curty, B. Qi, *Phys. Rev. Lett.* **2012**, *108*, 130503.
- [248] A. Rubenok, J. A. Slater, P. Chan, I. Lucio-Martinez, W. Tittel, *Phys. Rev. Lett.* **2013**, *111*, 130501.
- [249] Y. Liu, T.-Y. Chen, L.-J. Wang, H. Liang, G.-L. Shentu, J. Wang, K. Cui, H.-L. Yin, N.-L. Liu, L. Li, X. Ma, J. S. Pelc, M. M. Fejer, C.-Z. Peng, Q. Zhang, J.-W. Pan, *Phys. Rev. Lett.* **2013**, *111*, 130502.
- [250] Y.-L. Tang, H.-L. Yin, S.-J. Chen, Y. Liu, W.-J. Zhang, X. Jiang, L. Zhang, J. Wang, L.-X. You, J.-Y. Guan, D.-X. Yang, Z. Wang, H. Liang, Z. Zhang, N. Zhou, X. Ma, T.-Y. Chen, Q. Zhang, J.-W. Pan, *Phys. Rev. Lett.* **2014**, *113*, 190501.
- [251] Z. Tang, Z. Liao, F. Xu, B. Qi, L. Qian, H.-K. Lo, *Phys. Rev. Lett.* **2014**, *112*, 190503.
- [252] L. Comandar, M. Lucamarini, B. Fröhlich, J. Dynes, A. Sharpe, S.-B. Tam, Z. Yuan, R. Penty, A. Shields, *Nat. Photonics* **2016**, *10*, 312.
- [253] H.-L. Yin, T.-Y. Chen, Z.-W. Yu, H. Liu, L.-X. You, Y.-H. Zhou, S.-J. Chen, Y. Mao, M.-Q. Huang, W.-J. Zhang, H. Chen, M. J. Li, D. Nolan, F. Zhou, X. Jiang, Z. Wang, Q. Zhang, X.-B. Wang, J.-W. Pan, *Phys. Rev. Lett.* **2016**, *117*, 190501.
- [254] C. Wang, Z.-Q. Yin, S. Wang, W. Chen, G.-C. Guo, Z.-F. Han, *Optica* **2017**, *4*, 1016.
- [255] H. Liu, W. Wang, K. Wei, X.-T. Fang, L. Li, N.-L. Liu, H. Liang, S.-J. Zhang, W. Zhang, H. Li, L. You, Z. Wang, H.-K. Lo, T.-Y. Chen, F. Xu, J.-W. Pan, *Phys. Rev. Lett.* **2019**, *122*, 160501.
- [256] B. Fröhlich, J. F. Dynes, M. Lucamarini, A. W. Sharpe, Z. Yuan, A. J. Shields, *Nature* **2013**, *501*, 69.
- [257] R. J. Hughes, J. E. Nordholt, K. P. McCabe, R. T. Newell, C. G. Peterson, R. D. Somma, arXiv:1305.0305, **2013**.
- [258] Y.-L. Tang, H.-L. Yin, Q. Zhao, H. Liu, X.-X. Sun, M.-Q. Huang, W.-J. Zhang, S.-J. Chen, L. Zhang, L.-X. You, Z. Wang, Y. Liu, C.-Y. Lu, X. Jiang, X. Ma, Q. Zhang, T.-Y. Chen, J.-W. Pan, *Phys. Rev. X* **2016**, *6*, 011024.



Liangliang Lu received his B.S. degree from Guangzhou University in 2009 and Ph.D. degree from Nanjing University (NJU) in 2015. He worked as a researcher in School of Physics, NJU from 2017 to 2020 and joined the School of Physical Science and Technology at Nanjing Normal University in November 2020. His research area is integrated photonic quantum information processing, including quantum simulation, quantum key distribution, and nonlinear optics.



Yanqing Lu received his B.S. and Ph.D. degrees from Nanjing University, China, in 1991 and 1996, respectively. He has 5 years of experience in the U.S. and China telecomm industries. He designed and developed a serial of liquid-crystal-based fiber-optic devices with his colleagues, which include variable optical attenuators, variable Mux/Demux, and DWDM wavelength blockers. He is currently a Changjiang Distinguished Professor at Nanjing University. His research interests include liquid crystal photonics, nonlinear optics and quantum optics.



Shining Zhu is a professor at the School of Physics and a principal investigator at the National Laboratory of Solid State Microstructures, Nanjing University (NJU), China. He is an academician of the Chinese Academy of Sciences, and a fellow of Optical Society of America, Chinese Optical Society, and American Physical Society, respectively. He got his master's and Ph.D. degrees from the Physics Department of NJU. Since then he has been working on functionally microstructured materials, paying close attention to their applications on laser, nonlinear and quantum optics. Due to his outstanding contributions, Professor Zhu and his colleagues received the First-Class State Natural Science Award in 2006.



Xiao-Song Ma received his B.S. degree from Nanjing University (NJU) in 2003 and Ph.D. degree from University of Vienna in 2010. He worked as a postdoc in University of Vienna and Yale University from 2010 to 2015, respectively. He joined the School of Physics, NJU as a professor in 2015. His research interests include quantum communication, quantum network, quantum simulation and computation, solid-state quantum memory, and integrated photonic quantum technologies.